Anthropogenic and Natural Causes for the Interannual Variation of PM_{2.5} in East Asia During Summer Monsoon Periods From 2008 to 2018

Danyang Ma¹, Min Xie^{1,2,*}, Huan He^{1,2}, Tijian Wang^{3,*}, Mengzhu Xi¹, Lingyun Feng¹, Shuxian Zhang¹, Shitong Chen¹

- 6 School of Environment, Nanjing Normal University, Nanjing 210023, China.
- 7 2 Carbon monitoring and digital application technology center, Carbon peak and carbon neutralization strategy
- 8 institute of Jiangsu Province, Nanjing 210023, China.

1

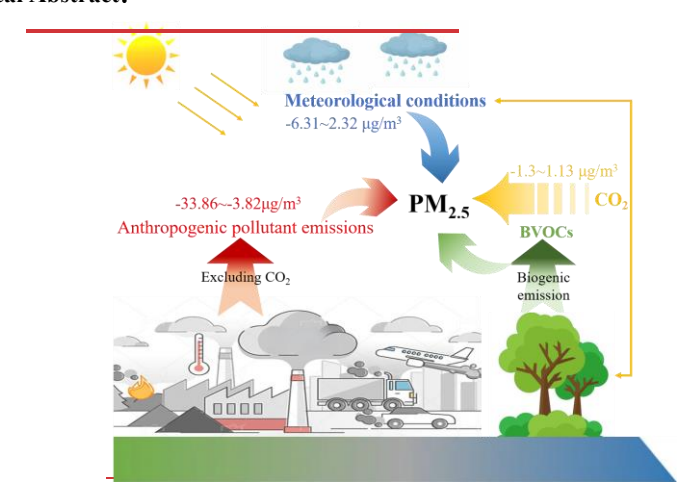
3

4

- 9 ³ School of Atmospheric Sciences, Nanjing University, Nanjing 210023, China.
- 10 Correspondence to: Min Xie(minxie@njnu.edu.cn); Tijian Wang (tjwang@nju.edu.cn)

Abstract. There was a significant difference in near-surface PM_{2.5} changes across China after the implementation of the Clean Air Action Plan in 2013. This study used the regional climatechemistry-ecosystem coupled model, RegCM-Chem-YIBs, to investigate interannual variations in PM2.5 across East Asia from 2008 to 2018. The drivers of PM2.5 variability were examined from Anthropogenic and Natural perspectives. Compared to 2008, PM_{2.5} showed little variation during 2009 2013 (the PreG phase (2009 2013)). However, during 2014 2018 (the PostG phase (2014–2018), a substantial decline in PM_{2.5} was simulated, particularly in the North China Plain (-36.76 μg/m³) and the Sichuan Basin (-33.96 μg/m³). Anthropogenic pollution pollution emissions were the primary drivers of PM_{2.5} reductions, contributing -10.39 to -3.82 μg/m³ in the PreG period and -33.86 to -8.45 μg/m³ in the PostG period. The influence of meteorological conditions on PM_{2.5} during the PreG phase (-6.31 to 2.32 µg/m³) was comparable to that of anthropogenic pollutant emissions. Additionally, in the vegetation-rich region, the impact of CO2 emission changes on PM_{2.5} was comparable to that of anthropogenic pollutant emissions. Our study comprehensively examined the drivers of PM2.5 concentration changes from 2008 to 2018. We highlight a significant intensification in the contribution of anthropogenic pollutant emissions and reveal that, in regions characterized by dense vegetation, changes in CO2 concentrations exert a pronounced impact on PM_{2.5} variations.

Graphical Abstract:



29

11

12

13

14 15

16 17

18

19 20

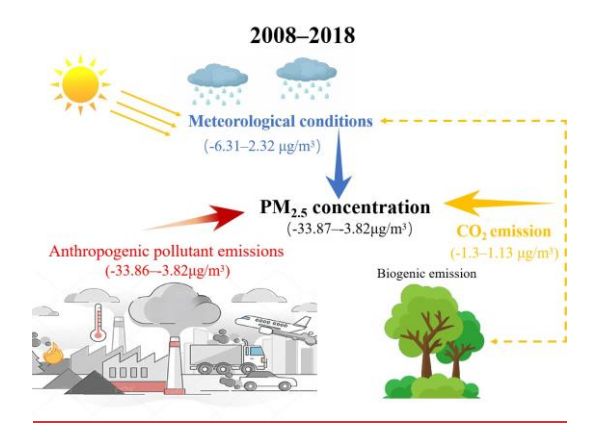
21

22

24

25

26



1 Introduction

PM2.5 refers to fine particulate matter with an aerodynamic diameter less than or equal to 2.5 micrometers (Chen et al., 2018). Its sources include industrial emissions, vehicular exhaust, biomass burning, and secondary formation from atmospheric gases (Wu et al., 2020). Major chemical components of PM2.5 include sulfates, nitrates, ammonium salts, organic carbon, elemental carbon, and heavy metals (Van Donkelaar et al., 2019; Li et al., 2017a). Fine particulate matter (PM2.5) is one of the primary atmospheric pollutants in China(Fontes et al., 2017), posing significant risks to human respiratory health(Feng et al., 2016; Xing et al., 2016). Long-term exposure to PM2.5 can lead to respiratory diseases such as chronic bronchitis, emphysema, and asthma(Kim et al., 2015; Pui et al., 2014; Xing et al., 2016). Additionally, PM2.5 is critical as a short-lived species influencing atmospheric radiation processes(Hu et al., 2017). It affects the radiative energy balance of the Earth-atmosphere system by scattering or reflecting solar radiation (direct effect)(Wu et al., 2021) and altering cloud microphysical properties (indirect effect)(Wang et al., 2018a; Wu et al., 2021).

With China's rapid economic development, widespread PM2.5 pollution became prevalent across the country in the early 21st century(Ma et al., 2016). In the most severely polluted urban areas, the annual average PM2.5 concentration exceeded 100 μ g/m³ (Van Donkelaar et al., 2010). From 2000 to 2008, the national average PM2.5 concentration in China was 49.4 ± 14.2 μ g/m³. In eastern China, the average concentration was 55.4 ± 16.1 μ g/m³, while the Beijing-Tianjin-Hebei region experienced average levels as high as 62.1 ± 22.5 μ g/m³. The Yangtze River Delta saw an average concentration of 63.0 ± 11.1 μ g/m³, the Pearl River Delta recorded an average of 52.4 ± 5.8 μ g/m³, and the Sichuan Basin averaged 61.6 ± 13.4 μ g/m³ (Wei et al., 2021). To mitigate the severe PM2.5 pollution, China implemented the Clean Air Action Plan in 2013(Li et al., 2019). This policy led to a significant nationwide decrease in PM2.5 concentrations(Zhang et al., 2019), marking a notable improvement in air quality ever since 2013 (Vu et al., 2019; Li et al., 2018).

The variation in $PM_{2.5}$ concentrations is influenced by three key factors: anthropogenic pollutant emissions, meteorological conditions(Xiao et al., 2021), and Carbon dioxide (CO₂) changes. Anthropogenic pollutant emissions encompass industrial production, transportation, and energy consumption(An et al., 2019), which release amounts of primary $PM_{2.5}$, as well as the precursors of secondary $PM_{2.5}$ such as volatile organic compounds (VOCs) (Kurokawa and Ohara, 2020) and nitrogen oxides (NO₈) (Wu et al., 2020; Zheng et al., 2021a; Kurokawa and Ohara, 2020). Consequently, reducing these emissions is essential for mitigating $PM_{2.5}$ concentrations, as they directly contribute to both the formation and persistence of particulate pollution(Zheng et al., 2018; Zhang et al., 2019).

Meteorological conditions play a significant role in influencing near-surface PM_{2.5} concentrations(Chen et al., 2020b; Xiao et al., 2021). Elevated temperatures can accelerate atmospheric chemical reactions(Mousavinezhad et al., 2021), including oxidation and photochemical processes, thereby promoting the formation of PM_{2.5} (Zhong et al., 2018). In addition, moderate increases in temperature can significantly enhance the emissions of biogenic volatile organic compounds (BVOCs) by stimulating the activity of the synthase enzyme. However, when temperatures exceed the physiological tolerance threshold of plants, decreased enzyme activity or metabolic disruption may suppress emissions(Lindwall et al., 2016; Kleist et al., 2012). Therefore, temperature changes can influence atmospheric PM_{2.5} concentrations by modulating the emissions of BVOCs. Precipitation aids in removing particulate matter from the atmosphere through wet deposition(Zhang et al., 2013), effectively reducing PM_{2.5} pollution

设置了格式: 下标

设置了格式: 上标

设置了格式: 下标

levels (Wu et al., 2018). Additionally, wind speed and direction are crucial factors in the transport and dispersion of particulate matter (Li et al., 2017b). Higher wind speeds facilitate the dispersion of particulate matter over a wider area, reducing its local accumulation and mitigating air pollution in specific regions (Li et al., 2017b; Zhang et al., 2018). The increase in planetary boundary layer height (PBLH) strengthens atmospheric upward motion(Ait-Chaalal et al., 2016), thereby reducing near-surface PM_{2.5} concentrations (Pan et al., 2019).

Changes in CO₂ concentrations can influence PM_{2.5} pollution levels through several mechanisms. Firstly, elevated CO2 concentrations impact the atmospheric radiation balance, altering the distribution and intensity of precipitation(Cao et al., 2012), which directly affects PM_{2.5} concentrations by influencing wet deposition rates(Zhang et al., 2022). Additionally, Changes in CO₂ concentrations can affect vegetation photosynthesis and growth, which alter the emissions of biogenic volatile organic compounds (BVOCs) that can participate in atmospheric chemical reactions to form secondary organic aerosols (SOA), and thereby impact atmospheric PM_{2.5} concentrations(Sun et al., 2013; Sun et al., 2012). It is worth noting that elevated CO₂ concentrations may also directly inhibit BVOCs emissions by reducing the activity of BVOCs synthase enzymes(Heald et al., 2009; Pegoraro et al., 2004). Therefore, the impact of increased CO₂ on vegetation BVOCs emissions can be either positive or negative, depending primarily on the relative strength of the inhibitory effect from enzyme suppression versus the stimulatory effect from enhanced photosynthesis(Sun et al., 2012). Isoprene is the most abundant species among BVOCs, so changes in CO₂ concentrations can indirectly affect near-surface PM_{2.5} concentrations by influencing isoprene emissions from vegetation(Sun et al., 2013; Lin et al., 2013; Kramer et al., 2016).

Numerous studies have used statistical models and numerical simulations to investigate the impacts of meteorological conditions and anthropogenic pollution emissions on PM_{2.5} concentration changes in China. The results consistently indicate that changes in anthropogenic pollution emissions are the primary driver of PM_{2.5} variation. Zhang et al. (2019) using the WRF-CMAQ model at the national scale, found that meteorological conditions accounted for only 9 % of the total decline in PM_{2.5} concentrations during 2013–2017 in China, suggesting that emission reductions were the dominant factor. Similarly, based on a multiple linear regression model, Chen et al. (2020a) reported that anthropogenic pollution emission reductions contributed 73 %, 87 %, and 84 % to the PM_{2.5} decline in the North China Plain, Yangtze River Delta, and Pearl River Delta, respectively, while the contribution of meteorological conditions ranged from 10 % to 26 %. Cheng et al. (2019) employing the WRF-CMAQ model, found that the decrease in PM_{2.5} concentrations in Beijing over the same period was mainly attributable to local (65.4 %) and regional (22.5 %) emission reductions, with meteorological conditions accounting for only 12.1 %.

Current research primarily emphasizes the impact of anthropogenic pollutant emissions (Zheng et al., 2018) and meteorological changes on PM_{2.5} concentrations (Zhang et al., 2019; Zhai et al., 2019), while the potential influence of CO₂ concentration changes on PM_{2.5} pollution levels remains largely underexplored. Additionally, following the implementation of the Clean Air Action Plan in 2013, significant decreases in PM_{2.5} concentrations were observed in China. Concurrently, CO₂ levels continued to rise(Xu et al., 2022), with the influence of CO₂ on PM_{2.5} strengthening annually. Therefore, it is essential to analyze the evolution of PM_{2.5} concentrations from 2008 to 2018 in detail, and attribute changes in PM_{2.5} levels to every factor, such as anthropogenic pollution emissions, meteorological conditions, and CO₂ variations.

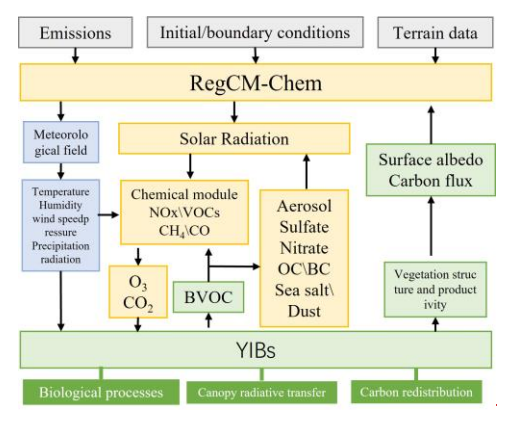
2 Methods and data

2.1 Model description

In this study, we employed the coupled regional climate-chemistry-ecology model RegCM-Chem-YIBs (Xie et al., 2019; Xie et al., 2024). The RegCM-Chem component simulates key meteorological variables, including temperature, humidity, precipitation, and radiation, along with atmospheric pollutants including ozone and particulate matter (Shalaby et al., 2012). The YIBs (Yale Interactive terrestrial Biosphere) model focuses on simulating vegetation physiological processes, such as ozone-induced damage, photosynthesis, and respiration(Lei et al., 2020). Additionally, it computes important land surface parameters, including CO₂ flux, biogenie volatile organic compound (BVOC) emissions, and stomatal conductance (Yue and Unger, 2015). The YIBs model employs a leaf-level BVOC emission scheme based on vegetation photosynthesis. Unlike the traditional MEGAN (Model of Emissions of Gases and Aerosols from Nature) model, this approach incorporates the influence of plant photosynthesis on BVOC emissions, making it more representative of actual plant physiological processes. In this scheme, leaf-level BVOC emission rates depend on the photosynthetic rate, leaf surface temperature, and intracellular CO₂ concentration (Yue and Unger, 2015; Lei et al., 2020; Yue et al., 2015).

The RegCM-Chem and YIBs models exchange variables every 6 minutes, facilitating dynamic coupling between regional climate, atmospheric chemistry, and ecosystem processes. The RegCM-Chem-YIBs model simulated both primary and secondary PM2.5 emissions, including dust, black carbon, organic carbon, sulfates, nitrates, and ammonium. The structure of the model is shown in Fig. 1.

In the RegCM-Chem-YIBs model, changes in CO₂ concentrations affect PM_{2.5} primarily viatow mechanisms: first, CO₂-induced radiative forcing alters the atmospheric radiation balance, leading to shifts in temperature, precipitation, and boundary - layer structure that modulate PM_{2.5} formation, transport, and removal(Li and Mölders, 2008; Matthews, 2007); And second, through the YIBs module, changes in CO₂ concentration modulate photosynthetic activity and stomatal behavior, altering BVOCs emissions that undergo atmospheric photochemical oxidation to form secondary organic aerosols, a significant fraction of PM_{2.5} (Kergoat et al., 2002; Kellomaki and Wang, 1998).



设置了格式: 下标

设置了格式: 下标
设置了格式: 下标
带格式的: 缩进: 首行缩进: 2 字符
设置了格式: 下标
设置了格式: 下标
设置了格式: 下标

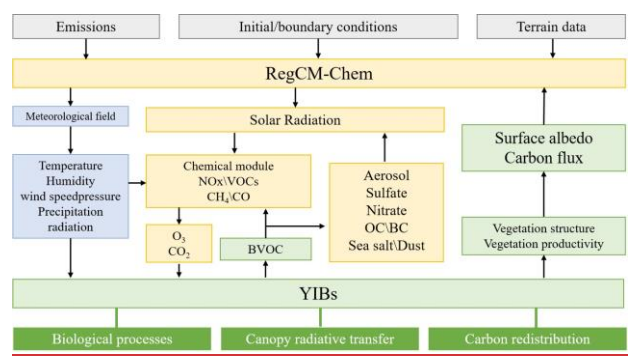


Figure 1. Framework of the RegCM-Chem-YIBs Model.

2.2 Model configurations

The study area covers the entire East Asian region, with a horizontal grid resolution of 60 km, centered at 36°N and 107°E. A terrain-following coordinate system was used vertically(Bleck and Benjamin, 1993), dividing the atmosphere into 18 layers from the surface to 50 hPa.

Anthropogenic pollutant emissions data were obtained from the Multi-resolution Emission Inventory for China (MEIC v1.4) developed by Tsinghua University(Geng et al., 2024). Surface CO₂ flux data were sourced from the National Oceanic and Atmospheric Administration (NOAA) CarbonTracker CT2019 dataset, which includes contributions from fossil fuel combustion, biomass burning, and ocean-atmosphere CO₂ exchange(Peters et al., 2007). Meteorological fields were derived from ERA-Interim reanalysis(Balsamo et al., 2015), while sea surface temperature data were taken from NOAA's weekly mean dataset(Huang et al., 2021). The model employed the Grell cumulus parameterization scheme, CCM3 radiation scheme, Holtslag PBL scheme for boundary layers, CBM-Z mechanism for meteorology and chemistry, and TUV photochemistry scheme.

2.3 Experiment settings

The numerical experiments are presented in Table 1. The SIM₂₀₀₈ experiment represents the baseline conditions for the year 2008. In the SIM_{pase} experiment, interannual variations in meteorological fields, CO₂ emissions, and anthropogenic pollutant emissions (excluding CO₂ emissions) were considered for simulations spanning 2008–2018, representing the baseline conditions for 2009–2018. The SIM_{Base} experiment accounted for interannual variations in meteorological fields, CO₂ emissions, and anthropogenic pollutant emissions (excluding CO₂) from 2008 to 2018. Additionally, the SIM_{MET=2008} and SIM_{CO2=2008} experiments were designed, where meteorological fields and CO₂ emissions were fixed at their 2008 levels, respectively, while simulations were conducted for 2009–2018. The simulation period spans from April to August each year. Among them, the results from May to August, corresponding to the East Asian Summer Monsoon (EASM) period, were selected for analysis.

Changes in PM_{2.5} concentrations were attributed to three main factors: anthropogenic pollution emissions, meteorological conditions, and CO₂ variations. By comparing the simulation

设置了格式: 下标 设置了格式: 下标 设置了格式: 下标 results from different years in the SIM_{Base} experiment to those from 2008SIM₂₀₀₈, we quantified changes in PM_{2.5} concentrations relative to 2008 for the period 2009–2018. To evaluate the impact of meteorological conditions on PM_{2.5} concentrations, we compared the results of the SIM_{Base} experiment with those of the SIM_{MET=2008} experiment for the same year (SIM_{Base} - SIM_{MET=2008}). Similarly, the contribution of CO₂ emission changes to PM_{2.5} variations was assessed by comparing the SIM_{Base} experiment with the SIM_{CO2=2008} experiment (SIM_{Base} - SIM_{CO2=2008}) in the same year. The contribution of anthropogenic pollutant emissions was then determined by subtracting the effects of meteorological and CO₂ emission changes from the total PM_{2.5} variation.

It is noteworthy that, as a principal greenhouse gas, CO_2 modifies meteorological parameters—such as radiation, temperature, and precipitation—which in turn influence PM_2 .5 levels. In this comparison, all meteorological changes derive solely from variations in CO_2 emissions, a mechanism fundamentally different from the meteorological influences identified in experiments SIM_{Base} and $SIM_{MET=2008}$.

Table 1. The Numerical experimental in this study.

Experiment	<u>Time</u>	Meteorological fields	CO ₂ emissions	Anthropogenic pollutant emissions
SIM ₂₀₀₈	2008	<u>2008</u>	2008	2008
SIM _{Base}	<u>2009-2018</u>	<u>2009-2018</u>	<u>2009-2018</u>	<u>2009-2018</u>
<u> </u>				
$SIM_{MET=2008}$	<u>2009-2018</u>	<u>2008</u>	<u>2009-2018</u>	<u>2009-2018</u>
<u>SIM</u> _{CO2=2008}	<u>2009-2018</u>	<u>2009-2018</u>	<u>2008</u>	<u>2009-2018</u>

—2.4 Model evaluations

185

186 187

188 189

> 190 191

192

193

194

195

196

197 198

199 200

201

202

203

204

205

206

207

208

209

210

211

212

213

214 215

216

217

218

219

220 221 Observed PM_{2.5} data were obtained from the China National Environmental Monitoring Center (CNEMC). This study used hourly PM_{2.5} concentrations during the summer monsoon period (May 1 to August 31) from 2015 to 2018. A total of 366 monitoring stations across Chinese cities, selected based on data completeness and representativeness, were used for model validation. The locations of these stations are shown in Fig. S5. CO₂ observations were sourced from the World Data Centre for Greenhouse Gases (WDCGG), including all seven sites in East Asia: Waliguan, Korea Tae-ahn Peninsula, Ulaanbaatar in Mongolia, Lulin, Yonagunijima, Cape D'Aguilar (Hong Kong), and King's Park. Detailed station locations are shown in Fig. S6. Reanalysis data for temperature, wind fields, and relative humidity were obtained from the ERA-Interim dataset.

The numerical experiments in this study follow the same design(Ma et al., 2023a) as in previous research. As shown in Table 2 and Figures S1–S6, the SIM_{Base} experiments reproduce 2015–2018 PM_{2.5} and CO₂ concentrations with high correlations and low biases relative to observations, while their simulated meteorological fields closely match reanalysis data. Therefore, the detailed parameterization schemes, settings, and model validation are provided in earlier publications and will not be repeated here. Overall, the RegCM-Chem-YIBsR model effectively captures the fundamental characteristics and temporal trends of simulates meteorological factors, PM_{2.5}, and CO₂ concentrations in East Asia(Ma et al., 2023a; Ma et al., 2023b).

设置了格式: 下标

设置了格式: 下标 设置了格式: 下标

设置了格式: 下标

设置了格式: 下标

设置了格式: 下标

设置了格式:字体:五号

设置了格式:字体:五号

设置了格式:字体:五号

设置了格式:字体:五号

设置了格式:字体:五号

设置了格式:字体:五号

设置了格式:字体:五号

带格式的:段落间距段前:0磅

带格式的: Heading-Secondary, 左, 2 级, 缩进: 左侧: 0 厘 米, 悬挂缩进: 3.57 字符, 首行缩进: 0 字符, 段落间距段 前: 0 磅, 多级符号 + 级别: 2 + 编号样式: 1, 2, 3, ... + 起始 编号: 1 + 对齐方式: 左侧 + 对齐位置: 0 厘米 + 缩进位 置: 0.63 厘米, 孤行控制

设置了格式: 下标 设置了格式: 下标

设置了格式: 下标

223

Table 2. Evaluations of the near-surface CO2 and PM2.5 in East Asia.

Species	<u>Year</u>	Observation	Simulation	<u>Bias</u>	RMSE	<u>R</u>	4
	2015	<u>402.82</u>	<u>406.98</u>	<u>4.16</u>	<u>9.37</u>	0.44	
CO. (nnm)	<u>2016</u>	<u>407.12</u>	<u>410.44</u>	<u>3.32</u>	8.22	0.69	
CO ₂ (ppm)	<u>2017</u>	408.35	413.62	<u>5.27</u>	<u>11</u>	<u>0.39</u>	-
	2018	<u>409.61</u>	<u>416.68</u>	<u>7.07</u>	11.32	0.41	
	<u>2015</u>	<u>48.77</u>	<u>44.75</u>	<u>-4.02</u>	29.39	0.57	
$MDA8 O_3$	<u>2016</u>	<u>50.16</u>	<u>46.95</u>	<u>-3.21</u>	27.56	0.60	4
(ppb)	2017	<u>55.43</u>	<u>51.87</u>	<u>-3.56</u>	21.55	0.74	
	<u>2018</u>	<u>55.53</u>	<u>52.08</u>	<u>-3.42</u>	<u>24.78</u>	0.73	
	2015	<u>36.6</u>	<u>25.57</u>	<u>-11.03</u>	12.99	0.71	
$PM_{2.5}$	<u>2016</u>	31.03	22.91	<u>-8.12</u>	10.31	0.64	4
(ug/m^3)	2017	<u>29.61</u>	24.02	<u>-5.59</u>	10.57	0.71	
	2018	27.18	19.04	-8.14	11.62	0.61	

RMSE: root mean square error; R: correlation coefficient.

224 225 226

227228

229

230

231

232

233

234

235236

237

238 239

240

241

242

243

244

245

Table 1. The Numerical experimental in this study

Experiment	Time	Meteorological fields	CO ₂ emissions	Anthropogenic pollutant emissions
SIM _{Base}	2008-2018	Varying	Varying	Varying
SIM _{MET=2008}	2009 2018	2008	Varying	Varying
SIM _{CO2=2008}	2009 2018	Varying	2008	Varying

3 Results and discussion

3.1 PM_{2.5} variation

Changes in PM_{2.5} concentrations from 2009 to 2018 relative to 2008 were quantified by comparing simulation results from each year in the SIM_{Base} experiment with SIM₂₀₀₈ (SIM_{Base} -SIM₂₀₀₈). Figure 2 illustrates the changes in near-surface PM_{2.5} concentrations across East Asia from 2009 to 2018. PM2.5 concentrations are notably higher in the North China Plain, northeastern China, and eastern China (Shanghai, Jiangsu, Zhejiang), largely driven by industrial emissions, vehicle exhaust, coal combustion, and dust from human activities (Wang et al., 2017). In contrast, regions in western China (Yunnan, Gansu, Xinjiang) exhibit lower PM_{2.5} levels due to limited industrial activity, lower population density, and more favorable meteorological conditions (Low water vapor content, lower temperatures, and weak solar radiation are unfavorable for the formation of secondary aerosols such as sulfates, nitrates, and organic aerosols)(Wei et al., 2021; Xue et al., 2020). Developed cities and industrial centers like the Pearl River Delta and Fuzhou (Fujian Province) continue encountering challenges related to PM2.5 pollution. Moreover, the Sichuan region, characterized by its enclosed basin geography and high population density, also experiences high PM_{2.5} pollution levels (Wang et al., 2018b). From 2009 to 2013, PM_{2.5} concentrations in China remained relatively stable, with levels averaging around 90 µg/m³ in the North China Plain and Sichuan Basin. However, following the implementation of the Clean Air Action Plan in 2013, PM_{2.5} levels significantly declined nationwide. By 2018, concentrations had dropped to below 50 µg/m³ across much of the country.

带格式的: 段落间距段前: 0 磅

设置了格式:字体:五号 设置了格式:字体:五号 带格式的:居中,段落间距段前:0磅

设置了格式:字体:五号

带格式的: 居中, 段落间距段前: 0磅

设置了格式:字体:五号

带格式的: 居中, 段落间距段前: 0磅

设置了格式: 字体: 五号

带格式的: 居中, 段落间距段前: 0 磅

设置了格式: 字体: 五号

带格式的: 段落间距段前: 0磅

设置了格式: 下标 设置了格式: 下标

设置了格式: 下标

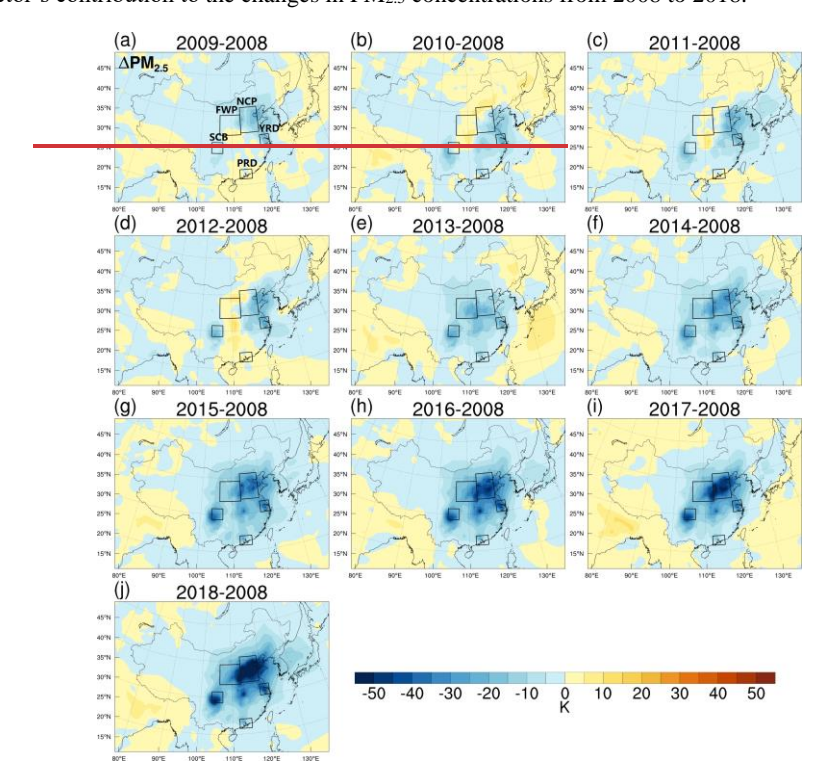
Figure 2. Near-surface PM_{2.5} concentrations (μg/m³) over East Asia during the EASM period May to August from 2009 (a) to 2018 (k) (SIM₂₀₀₈). Key regions are highlighted by black boxes, including the North China Plain (NCP), Fenwei Plain (FWP), Yangtze River Delta (YRD), Pearl River Delta (PRD), and Sichuan Basin (SCB).

 Figure 3 and Table 351 present the changes in PM2.5 concentrations relative to 2008 across East Asia from 2009 to 2018. Since 2008, most regions in China have seen varying degrees of PM2.5 reduction. During the pre-governance period (PreG, 2009~2013), the largest decrease occurred in the Yangtze River Delta, with a reduction of 14.77 μ g/m³, followed by the Sichuan Basin and Pearl River Delta, where concentrations dropped by 10.59 μ g/m³ and 8.69 μ g/m³, respectively. In contrast, the Fenwei Plain and Pearl River Delta experienced smaller changes, with reductions of less than 3 μ g/m³. PM2.5 concentrations across China significantly decreased after the implementation of the Clean Air Action Plan in 2013. The most notable reductions were simulated in the North China Plain and Sichuan Basin, where PM2.5 concentrations dropped by 36.76 μ g/m³ and 33.96 μ g/m³, respectively. In the Fenwei Plain and Yangtze River Delta, PM2.5 concentrations decreased by 22.16 to 27.89 μ g/m³. In contrast, the Pearl River Delta saw a smaller reduction, with levels decreasing by just 8.03 μ g/m³. This may be attributed to the region's significant influence from the summer monsoon and relatively lower impact from anthropogenic pollution emissions. Further analysis of these factors will be conducted in subsequent sections.

设置了格式:字体:五号 设置了格式:下标 设置了格式:字体:五号

Table S1 shows that the mean PM_{2.5} trend over China during the PreG (2009-2013) and PostG (2014-2018) periods was −1.84 μg/m³/yr and −2.90 μg/m³/yr, respectively. These values are consistent with the findings of Silver et al. (2025), who reported a PM_{2.5} trend of −2.47 μg/m³/yr for 2014–2017 in China based on ground-based observations. Similarly, Lin et al. (2018) reported PM_{2.5} trends of −0.65 and −2.30 μg/m³/yr for 2006–2010 and 2011–2015 in China, respectively. Using satellite remote sensing data, Ma et al. (2019) found declines of 1.03 and 4.27 μg/m³/yr for 2010-2013 and 2013-2017 in China, respectively. The high-resolution Chinese air quality reanalysis (CAQRA), developed by Kong et al. (2021) using data assimilation techniques, indicated a more pronounced decline of −5.80 μg/m³/yr for PM_{2.5} from 2013 to 2018 in China. In addition, Silver et al. (2018), based on multi-source data, reported a trend of −3.40 μg/m³/yr for 2015–2017 in China. Therefore, our simulation accurately captures the observed PM_{2.5} trends over China from 2008 to 2018, providing a robust foundation for subsequent attribution analyses.

Overall, before 2013, near-surface PM_{2.5} concentrations across China showed little variation. However, after 2013, a significant reduction in PM_{2.5} pollution levels was simulated nationwide. Changes in PM_{2.5} concentrations were attributed to three main factors: anthropogenic pollution emissions, meteorological conditions, and CO₂ variations. The following sections analyze each factor's contribution to the changes in PM_{2.5} concentrations from 2008 to 2018.



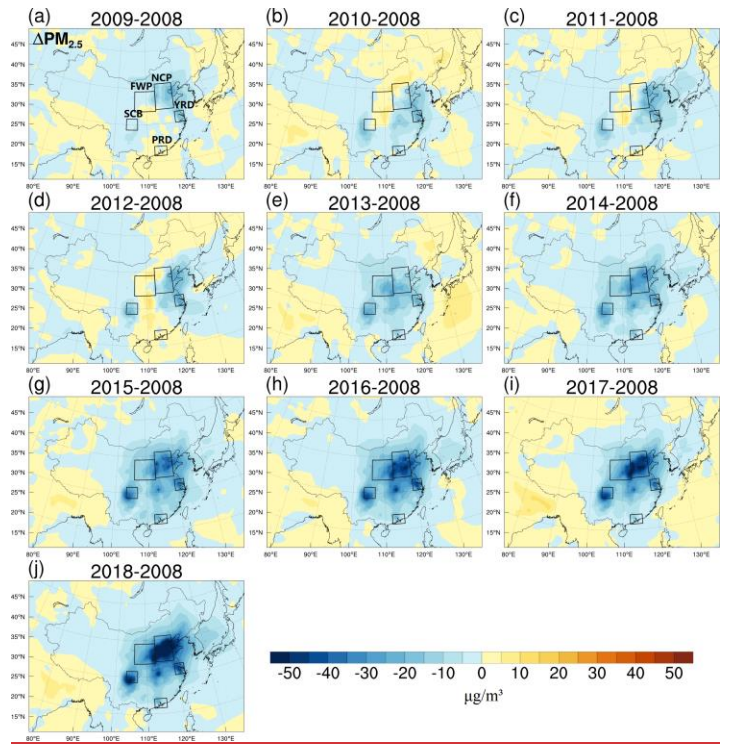


Figure 3. Changes in near-surface PM_{2.5} concentrations (μg/m³) during the EASM period May to August from 2009 (a) to 2018 (j) relative to 2008 in East Asia (SIM_{Base} - SIM₂₀₀₈).

Table 3. Changes in near-surface PM_{2.5} concentrations (μg/m³) during the EASM period from 2009 to 2018 relative to 2008 in the North China Plain (NCP), Fen-Wei Plain (FWP), Yangtze River Delta (YRD), Pearl River Delta (PRD), and Sichuan Basin (SCB) (SIM_{Base} - SIM₂₀₀₈).

Year NCP FWP YRD PRD SCB 2009 -11.24 -1.29 -11.37 1.41 -3.16 4 2010 -3.87 1.9 -15.2 -3.57 -4.79 4 2011 -6.27 0.22 -14.76 0.13 -8.65 4 2012 -7.42 1.69 -17.61 2.35 -15.99 4 2013 -14.67 -15.49 -14.9 -6.34 -20.37 4 2014 -24.26 -15.36 -19.95 -6.72 -22.87 4 2015 -31.41 -16.9 -27.76 -9.91 -31.75 4 2016 -38.5 -25.23 -32.43 -8.18 -35.58 4 2017 -40.69 -25.49 -26.21 -5.82 -37.43 4 2018 -48.96 -27.83 -33.08 -9.53 -42.19 4 PreG -8.69 -2.59 -14.77 -1.20	Ittivet Detta (III	CD /, und Diendun D	dom (DCD) (Divibase	D1111 2000 1.		
2010 -3.87 1.9 -15.2 -3.57 -4.79 2011 -6.27 0.22 -14.76 0.13 -8.65 2012 -7.42 1.69 -17.61 2.35 -15.99 2013 -14.67 -15.49 -14.9 -6.34 -20.37 2014 -24.26 -15.36 -19.95 -6.72 -22.87 2015 -31.41 -16.9 -27.76 -9.91 -31.75 2016 -38.5 -25.23 -32.43 -8.18 -35.58 2017 -40.69 -25.49 -26.21 -5.82 -37.43 2018 -48.96 -27.83 -33.08 -9.53 -42.19 PreG -8.69 -2.59 -14.77 -1.20 -10.59	Year	<u>NCP</u>	<u>FWP</u>	YRD	<u>PRD</u>	<u>SCB</u>
2010 -3.87 1.9 -15.2 -3.57 -4.79 2011 -6.27 0.22 -14.76 0.13 -8.65 2012 -7.42 1.69 -17.61 2.35 -15.99 2013 -14.67 -15.49 -14.9 -6.34 -20.37 2014 -24.26 -15.36 -19.95 -6.72 -22.87 2015 -31.41 -16.9 -27.76 -9.91 -31.75 2016 -38.5 -25.23 -32.43 -8.18 -35.58 2017 -40.69 -25.49 -26.21 -5.82 -37.43 2018 -48.96 -27.83 -33.08 -9.53 -42.19 PreG -8.69 -2.59 -14.77 -1.20 -10.59	2009	<u>-11.24</u>	<u>-1.29</u>	<u>-11.37</u>	<u>1.41</u>	<u>-3.16</u>
2011 -6.27 0.22 -14.76 0.13 -8.65 2012 -7.42 1.69 -17.61 2.35 -15.99 2013 -14.67 -15.49 -14.9 -6.34 -20.37 2014 -24.26 -15.36 -19.95 -6.72 -22.87 2015 -31.41 -16.9 -27.76 -9.91 -31.75 2016 -38.5 -25.23 -32.43 -8.18 -35.58 2017 -40.69 -25.49 -26.21 -5.82 -37.43 2018 -48.96 -27.83 -33.08 -9.53 -42.19 PreG -8.69 -2.59 -14.77 -1.20 -10.59	<u>2010</u>	<u>-3.87</u>	<u>1.9</u>	<u>-15.2</u>	<u>-3.57</u>	<u>-4.79</u>
2013 -14.67 -15.49 -14.9 -6.34 -20.37 2014 -24.26 -15.36 -19.95 -6.72 -22.87 2015 -31.41 -16.9 -27.76 -9.91 -31.75 2016 -38.5 -25.23 -32.43 -8.18 -35.58 2017 -40.69 -25.49 -26.21 -5.82 -37.43 2018 -48.96 -27.83 -33.08 -9.53 -42.19 PreG -8.69 -2.59 -14.77 -1.20 -10.59	<u>2011</u>	<u>-6.27</u>	<u>0.22</u>	<u>-14.76</u>	0.13	<u>-8.65</u>
2013 -14.67 -15.49 -14.9 -6.34 -20.37 2014 -24.26 -15.36 -19.95 -6.72 -22.87 2015 -31.41 -16.9 -27.76 -9.91 -31.75 2016 -38.5 -25.23 -32.43 -8.18 -35.58 2017 -40.69 -25.49 -26.21 -5.82 -37.43 2018 -48.96 -27.83 -33.08 -9.53 -42.19 PreG -8.69 -2.59 -14.77 -1.20 -10.59	<u>2012</u>	<u>-7.42</u>	<u>1.69</u>	<u>-17.61</u>	2.35	<u>-15.99</u>
2017 -40.69 -25.49 -26.21 -5.82 -37.43 -37.43 2018 -48.96 -27.83 -33.08 -9.53 -42.19 PreG -8.69 -2.59 -14.77 -1.20 -10.59	<u>2013</u>	<u>-14.67</u>	<u>-15.49</u>	<u>-14.9</u>	<u>-6.34</u>	<u>-20.37</u>
2017 -40.69 -25.49 -26.21 -5.82 -37.43 -37.43 2018 -48.96 -27.83 -33.08 -9.53 -42.19 PreG -8.69 -2.59 -14.77 -1.20 -10.59	<u>2014</u>	<u>-24.26</u>	<u>-15.36</u>	<u>-19.95</u>	<u>-6.72</u>	<u>-22.87</u>
2017 -40.69 -25.49 -26.21 -5.82 -37.43 -37.43 2018 -48.96 -27.83 -33.08 -9.53 -42.19 PreG -8.69 -2.59 -14.77 -1.20 -10.59	<u>2015</u>	<u>-31.41</u>	<u>-16.9</u>	<u>-27.76</u>	<u>-9.91</u>	<u>-31.75</u>
2017 -40.69 -25.49 -26.21 -5.82 -37.43 4 2018 -48.96 -27.83 -33.08 -9.53 -42.19 4 PreG -8.69 -2.59 -14.77 -1.20 -10.59	<u>2016</u>	<u>-38.5</u>	<u>-25.23</u>	<u>-32.43</u>		<u>-35.58</u>
<u>PreG</u> -8.69 -2.59 -14.77 -1.20 -10.59	<u>2017</u>	<u>-40.69</u>	<u>-25.49</u>	<u>-26.21</u>	<u>-5.82</u>	<u>-37.43</u>
PreG -8.69 -2.59 -14.77 -1.20 -10.59 PostG -36.76 -22.16 -27.89 -8.03 -33.96	<u>2018</u>	<u>-48.96</u>	<u>-27.83</u>	<u>-33.08</u>	<u>-9.53</u>	
<u>PostG </u>	<u>PreG</u>	<u>-8.69</u>				<u>-10.59</u>
	<u>PostG</u>	<u>-36.76</u>	<u>-22.16</u>	<u>-27.89</u>	<u>-8.03</u>	<u>-33.96</u>

3.2 Contribution of meteorological conditions

289 290

291

292

293 294 295

296

297

设置了格式:字体:五号 设置了格式:字体:五号

 带格式的: 居中

 带格式的: 居中

The impact of meteorological conditions variations on PM_{2.5} concentrations were assed by compared SIM_{pase} results with those from SIM_{MET=2008} for the same year (SIM_{pase} - SIM_{MET=2008}). As shown in Fig. 4, during the PreG period, the precipitation increased by 2–4 mm/day in China's eastern coastal and western inland regions, while it decreased by approximately 2 mm/day in central China. This increase in precipitation facilitates the reduction of near-surface PM_{2.5} concentrations through wet deposition. Consequently, trends in PM_{2.5} concentrations are inversely related to precipitation: concentrations decreased by 2–16 μg/m³ in the eastern coastal and western inland regions, while increased by 4–8 μg/m³ around 110°E in central China. Additionally, in northeastern and southwestern China, wind speeds increased by 1 to 2 m/s, contributing to the reduction of PM_{2.5} concentrations. In contrast, decreased wind speeds in southeastern and central China facilitated the accumulation of PM_{2.5}. During the PostG period, the significant increase in temperature (Fig. 4l) promoted the formation of PM_{2.5}, leading to an expansion of the areas where PM_{2.5} concentrations increased. Overall, PM_{2.5} concentrations have decreased in the eastern coastal and western inland regions but increased in the central area of China.

Table 482 indicates that in the NCP region, precipitation increased by 0.58 to 0.6 mm/day, and wind speed rose by 0.17 to 0.26 m/s during the PreG and PostG periods, resulting in a decrease in near-surface PM_{2.5} concentrations of 1.6 to 4.01 μg/m³. In the FWP region, PM_{2.5} concentrations increased by 1 to 2.31 μg/m³, which was associated with a rise in temperature of 0.1 to 0.46 K and a significant decrease in PBLH of 108.5 to 15.3 m. In the YRD region, the increase in wind speed of 0.48 to 1.02 m/s facilitated a reduction in PM_{2.5} concentrations by 0.43 to 0.61 μg/m³. Conversely, in the PRD region, reduced precipitation combined with increased temperature contributed to an increase in PM_{2.5} concentrations, ranging from 0.11 to 1.49 μg/m³. In the SCB region, PM_{2.5} concentrations rose by 0.29 μg/m³ during the PreG period, linked to a significant decrease in PBL height of 136.5 m. In the PostG period, PM_{2.5} concentrations decreased by 1.14 μg/m³, attributed to an increase in precipitation (0.37 mm/day) and a decrease in temperature (0.14 K).

设置了格式: 下标 设置了格式: 下标 设置了格式: 下标

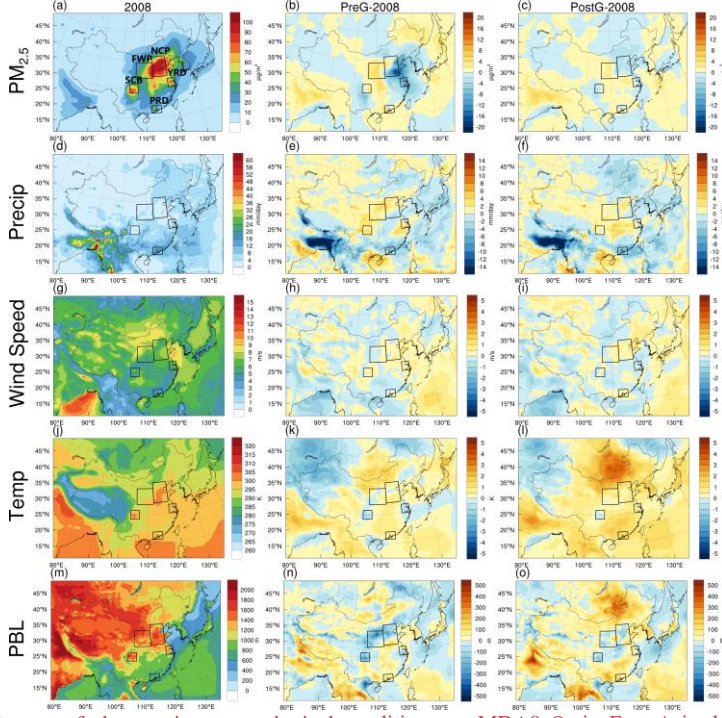


Figure 4. Impact of changes in meteorological conditions on MDA8 O₃ in East Asia during May to August from 2009 (a) to 2018 (j). The PM_{2.5} (a-c, µg/m³), precipitation (d-f, mm/day), wind speed (g-i, m/s), temperature (k-l, K), and Planetary Boundary Layer (PBL) height (m-o, m) during the EASM period in 2008 (left), and their mean changes due to meteorological variations in PreG (2009–2013, center) and PostG (2014–2018, right) phase relative to 2008 (SIM_{Base} - SIM_{MET=2008})₄

Table 4. Impact of meteorological condition changes on PM_{2.5} (μg/m³), precipitation (mm/day), wind speed (m/s), near-surface temperature (K), and Planetary Boundary Layer (PBL) height (m) during the EASM period in PreG (2009–2013) and PostG (2014–2018) phase relative to 2008 (SIM₂₀₀₄ - SIM₂₀₀₇ - SI

Region	<u>Period</u>	$\frac{PM_{2.5}}{(\mu g/m^3)}$	Precipitation (mm/day)	Wind Speed (m/s)	Near-Surface Temperature (K)	<u>PBL</u> (m)
NCP	<u>PreG</u>	<u>-4.01</u>	0.58	0.17	0.32	<u>-46.8</u>
	<u>PostG</u>	<u>-1.6</u>	<u>0.6</u>	<u>0.26</u>	<u>0.6</u>	<u>-14.5</u>
<u>FWP</u>	<u>PreG</u>	2.32	1.68	<u>-0.06</u>	<u>0.1</u>	<u>-108.5</u>
1. AA 1	<u>PostG</u>	<u>1</u>	<u>0.81</u>	0.05	<u>0.46</u>	<u>-15.3</u>
YRD	<u>PreG</u>	<u>-6.31</u>	1.02	0.18	<u>-0.29</u>	<u>-33.9</u>
	<u>PostG</u>	-0.43	0.48	-0.08	0.45	21.9
PRD	PreG	1.49	-2.39	-0.02	0.36	29.6
	<u>PostG</u>	0.11	<u>-3.24</u>	0.18	1.00	<u>52.2</u>
SCD	PreG	0.29	1.81	0.13	-0.58	<u>-136.5</u>
<u>SCB</u>	<u>PostG</u>	<u>-1.14</u>	<u>0.37</u>	<u>-0.03</u>	<u>-0.14</u>	<u>-76</u>

→ 设置了格式:字体:五号

3.3 Contribution of CO₂

The contribution of CO₂ emission changes to PM_{2.5} variability was quantified by comparing the SIM_{Base} experiment with the SIM_{CO2=2008} experiment (SIM_{Base} - SIM_{CO2=2008}) within the same year. As shown in Fig. 5, Following the ongoing urbanization and industrialization, CO₂ concentrations across East Asia rose by 2–10 ppm during both the PreG and PostG periods, with a sharper increase in the PostG period. CO₂ influences atmospheric PM_{2.5} concentrations both through its radiative effects on precipitation and by altering BVOCs emissions from vegetation. Overall, CO₂ changes contributed to PM_{2.5} variations across East Asia from 2008 to 2018, ranging from -4 to 6 μg/m³. PM_{2.5} pollution levels generally increased in the PreG period, while reductions were more common in the PostG period.

Table 583 presents a detailed analysis of the five target regions. In northern China, particularly the NCP and FWP regions, limited vegetation coverage means CO2 impacts surface PM2.5 concentrations mainly through precipitation changes. In the PostG period, precipitation increased by 0.06–0.13 mm/day, lowering PM2.5 concentrations by 0.98–1.3 μg/m³. Similarly, in the Sichuan Basin, precipitation rose by 0.21–0.64 mm/day, reducing PM2.5 concentrations by 0.49–0.73 μg/m³ in the PreG and PostG period. However, in the YRD and PRD regions, where vegetation coverage is higher, CO2 primarily impacts PM2.5 concentrations by modulating BVOCs emissions. The impact can be either positive or negative(Possell et al., 2005), depending primarily on the balance between the inhibitory effects on synthase activity and the stimulatory effects of enhanced photosynthesis(Wilkinson et al., 2009). In the YRD region, isoprene fell by 0.32–0.58 μg/m³ during both periods, while precipitation rose by 0.09–0.13 mm/day, collectively reducing PM2.5 by 0.02–0.05 μg/m³. In the PRD region, isoprene concentrations increased significantly by 0.31–0.92 μg/m³, while precipitation decreased by 0.33–1.02 mm/day. Consequently, PM2.5 concentrations rose by 0.31–1.13 μg/m³ during both the PreG and PostG periods.

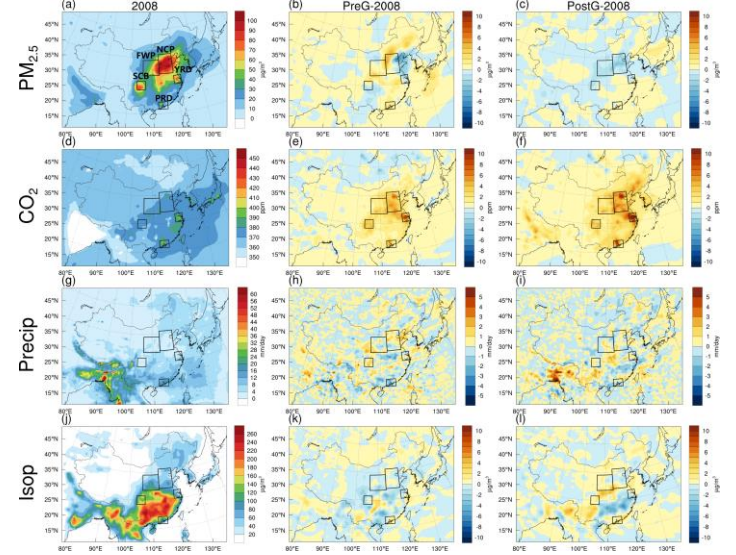


Figure 5. The PM_{2.5} (a-c, µg/m³), CO₂ (d-f, ppm), precipitation (g-i, mm/day), and isoprene (j-l, µg/m³)

设置了格式: 下标 设置了格式: 下标 设置了格式: 下标 设置了格式: 下标

设置了格式: 下标

> 369 370

371

372

during the EASM period in 2008 (left), and their mean changes due to CO₂ emission variations in PreG (2009–2013, center) and PostG (2014–2018, right) phase relative to 2008 (SIM_{Base} - SIM_{CO2-2008}). The impact of CO₂ concentration changes on PM_{2.5} (μg/m³), CO₂ (ppm), precipitation (mm/day), and isoprene (μg/m³).

Table 5. Impact of CO₂ emission changes on PM_{2.5} (μg/m³), CO₂ (ppm), precipitation (mm/day), and isoprene (μg/m³) during the EASM period in PreG (2009–2013) and PostG (2014–2018) phase relative to 2008 (SIM_{Base} - SIM_{CO2=2008}).

PM_{2.5} CO_2 **Precipitation** <u>Isoprene</u> Region Period $(\mu g/m^3)$ (mm/day) $(\mu g/m^3)$ (ppm) -0.1 **PreG** 0.6 3.19 0.27 NCP 4.24 0.26 **PostG** -1.3 0.13 0.21 **PreG** 0.84 1.70 -0.16 <u>FWP</u> <u>-0.98</u> 2.05 0.06 0.33 PostG **PreG** -0.02 4.1 0.13 -0.32**YRD** -0.05 0.09 **PostG** 6.2 <u>-0.58</u> **PreG** 1.13 1.97 -1.020.31 <u>PRD</u> **PostG** 0.31 3.20 -0.330.92 **PreG** -0.49 2.80 0.64 -0.78 **SCB** PostG -0.73 0.21 0.69

373 374 375

376 377

378

379

380

381

382

383

384

385

386

387 388 3.4 Contribution of anthropogenic pollutant emissions

The contribution of changed anthropogenic pollutant emissions to PM2.5 variation was determined by removing the effects of meteorological and CO2 emission changes from the total variation. Figure 6 illustrates a significant downward trend in PM2.5 concentrations across East Asia since 2008. During the PreG period, PM_{2.5} levels decreased by an average of 5 to 10 µg/m³ over East Asia. Following the implementation of the Clean Air Action Plan in 2013, a marked reduction in PM2.5 concentrations was simulated. The most substantial decreases occurred in the NCP and SCB region, with approximately 60 µg/m³. Anthropogenic pollutant emissions emerged as the primary drivers of this decline, with their spatial distribution and magnitude of impact closely corresponding to the overall changes in PM2.5 concentrations. In contrast, the effects of changing meteorological conditions and CO₂ concentrations emissions on PM_{2.5} levels in East Asia were relatively minor, ranging between -5 to 5 μg/m³. Meteorological conditions have reduced PM2.5 concentrations in the eastern coastal and western regions of China, while increasing them in the central region. In the PostG period, the extent of PM2.5 concentration increases has expanded. The impact of CO₂ concentration emission changes on PM_{2.5} levels shows different trends in the PreG and PostG periods. In the PreG period, changes in CO2 concentrations emissions primarily led to an increase in PM2.5 concentrations. However, in the PostG period, the rise in CO₂ concentrations began to have a negative impact, leading to a reduction in PM_{2.5} concentrations.

389 390 391

392

393

设置了格式: 下标

设置了格式: 下标

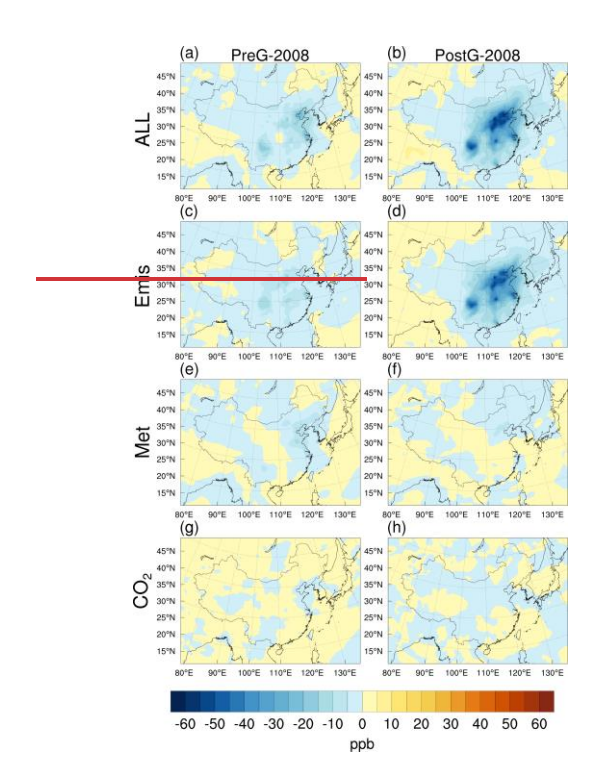


Figure 6. The total changes in PM_{2.5} concentrations in the East Asia region relative to 2008 (All, SIM_{Base} - SIM₂₀₀₈), and the changes in PM_{2.5} attributed to variations of anthropogenic pollutant emissions (Emis, All-Met-CO₂), meteorological conditions (Met, SIM_{Base} - SIM_{MET-2008}), and CO₂ concentrations emissions (CO₂, SIM_{Base} - SIM_{CO2-2008}) during the EASM period in PreG (2009–2013, left) and PostG (2014–2018, right) phase relative to 2008.

397

398

399

400

401

402

403

404

405

406

407

Based on Fig. 7 and Table $\underline{6}$ S4, PM_{2.5} concentrations in the NCP region decreased by 5.28 $\mu g/m^3$ during the PreG period and by 33.86 $\mu g/m^3$ in the PostG period. Anthropogenic pollution emissions were the primary driver of these changes. During the PreG period, the influence of meteorological conditions on PM_{2.5} was comparable to that of anthropogenic pollution emissions, with changes in meteorology contributing -4.01 $\mu g/m^3$ and emissions contributing -5.28 $\mu g/m^3$. However, in the PostG period, the impact of meteorological factors diminished to -1.6 $\mu g/m^3$,

设置了格式:字体:五号
设置了格式:字体:五号
设置了格式:字体:五号
设置了格式:字体:五号
设置了格式:字体:五号
设置了格式:字体:五号
设置了格式:字体:五号
设置了格式:字体:五号
设置了格式:字体:五号

indicating that anthropogenic pollution emissions became the predominant factor in the reduction of PM_{2.5} concentrations. In contrast, the effect of changes in CO₂ concentrations emissions on PM_{2.5} levels was relatively minor, ranging from -1.3 to $0.6 \mu g/m^3$.

The situation in the FWP region is similar to that of the NCP region, with anthropogenic pollution emissions as the primary driver of reduced PM_{2.5} concentrations. During the PreG and PostG periods, the contributions of anthropogenic pollution emissions to PM_{2.5} levels were -5.75 µg/m³ and -22.18 µg/m³, respectively. In contrast, meteorological conditions contributed to an increase in PM_{2.5} concentrations, with a contribution of 2.32 µg/m³ in the PreG period, comparable to the impact of anthropogenic pollution emissions. Meanwhile, the influence of CO₂ concentrations emissions on PM_{2.5} levels was relatively minor.

In the YRD region, anthropogenic <u>pollution</u> emissions are the primary driver of reduced PM_{2.5} concentrations. Due to its location in eastern China, the YRD region is more affected by the EASM, resulting in more pronounced effects of changing meteorological conditions on PM_{2.5} levels compared to the NCP and FWP regions. During the PreG period, the impact of meteorological conditions on PM_{2.5} concentrations reached as high as $-6.31 \,\mu\text{g/m}^3$.

In the PRD region, changes in anthropogenic pollution emissions have contributed to a reduction in PM_{2.5} concentrations, ranging from -8.45 to -3.82 μ g/m³. However, changes in meteorological conditions and CO₂ concentrations emissions have led to increases in PM_{2.5} levels, ranging from 0.11 to 1.49 μ g/m³. Similar to the YRD region, the effects of changing meteorological conditions on PM_{2.5} concentrations are significant, peaking at 1.49 μ g/m³ during the PreG period. Located in southeastern coastal China, the Pearl River Delta's rich vegetation cover enhances the impact of CO₂ emission changes on PM_{2.5} concentrations. During the PreG period, the influence of CO₂ concentration-emission changes on PM_{2.5} levels reached 1.13 μ g/m³, comparable to the effect of anthropogenic pollution emissions (-3.82 μ g/m³). In the PostG period, the impact of CO₂ emission changes (0.31 μ g/m³) surpassed that of meteorological conditions (0.11 μ g/m³).

In the SCB region, the basin topography results in relatively minor effects of meteorological conditions and CO₂ concentration emission changes on PM_{2.5} levels, with contributions ranging from -1.14 to 0.29 μg/m³ during both the PreG and PostG periods. In contrast, anthropogenic pollution emissions are the primary drivers of reduced PM_{2.5} concentrations, exerting an impact of -32.09 μg/m³ during the PostG period.

Page 19 of 29

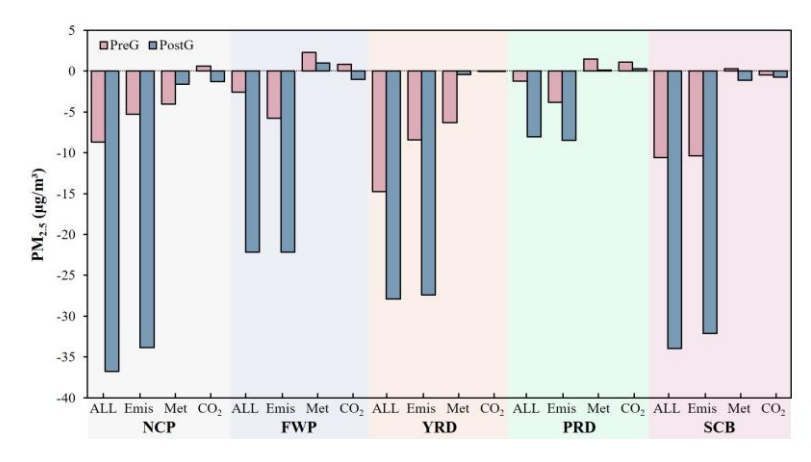


Figure 7. The total changes in PM_{2.5} concentrations (All, <u>SIM_{Base} - SIM₂₀₀₈</u>) for the North China Plain (NCP), Fenwei Plain (FWP), Yangtze River Delta (YRD), Pearl River Delta (PRD), and Sichuan Basin (SCB) <u>during the EASM period in PreG (2009–2013) and PostG (2014–2018) phase relative to 2008, along with the variations in PM_{2.5} due to anthropogenic pollutant emissions (Emis, <u>All-Met-CO₂</u>), meteorological conditions (Met, <u>SIM_{Base} - SIM_{MET-2008}</u>), and CO₂ <u>concentration emission</u> (CO₂, <u>SIM_{Base} - SIM_{CO2-2008}</u>) changes.</u>

Table 6. Changes in total PM_{2.5} concentrations (ALL, SIM_{Base} - SIM₂₀₀₈) and the impacts of anthropogenic pollutant emissions (Emis, All-Met-CO₂), meteorological conditions (Met, SIM_{Base} - SIM_{MET=2008}), and CO₂ emission (CO₂, SIM_{Base} - SIM_{CO2=2008}) variations on PM_{2.5} concentrations (μg/m³) during the EASM period in PreG (2009–2013) and PostG (2014–2018) phase relative to 2008.

1100 (200) 2010) a	marosto (Borr 2	oro, primbe return	0 10 20001			
Region	Period	ALL	<u>Emis</u>	Met	CO_2	
NCD	<u>PreG</u>	<u>-8.69</u>	<u>-5.28</u>	<u>-4.01</u>	0.6	
<u>NCP</u>	<u>PostG</u>	<u>-36.76</u>	-33.86	<u>-1.6</u>	<u>-1.3</u>	
EWD	PreG	<u>-2.59</u>	<u>-5.75</u>	2.32	0.84	
<u>FWP</u>	PostG	<u>-22.16</u>	-22.18	<u>1</u>	<u>-0.98</u>	
YRD	<u>PreG</u>	<u>-14.77</u>	<u>-8.44</u>	<u>-6.31</u>	<u>-0.02</u>	
	<u>PostG</u>	<u>-27.89</u>	<u>-27.41</u>	<u>-0.43</u>	<u>-0.05</u>	
PRD	<u>PreG</u>	<u>-1.2</u>	<u>-3.82</u>	<u>1.49</u>	<u>1.13</u>	
	<u>PostG</u>	<u>-8.03</u>	<u>-8.45</u>	<u>0.11</u>	<u>0.31</u>	
<u>SCB</u>	<u>PreG</u>	<u>-10.59</u>	<u>-10.39</u>	0.29	<u>-0.49</u>	
	PostG	-33.96	-32.09	-1.14	-0.73	

3.5 Attribution of Changes in PM_{2.5}

 Figure 8 illustrates that $PM_{2.5}$ concentrations remained relatively stable across the five regions during the PreG period. However, in the PostG period, following the implementation of the Clean Air Action Plan, significant reductions in $PM_{2.5}$ concentrations were simulated in the NCP, FWP, YRD, and SCB regions, while the PRD region showed the smallest decrease.

Anthropogenic pollutant emissions are the primary factor driving PM_{2.5} concentration reductions across the five regions, with their impact increasing linearly over time. In the PreG

设置了格式:字体:五号
设置了格式:字体:五号
设置了格式: 字体: 五号

period, meteorological conditions had a relatively stronger influence on $PM_{2.5}$ levels, occasionally surpassing the effects of anthropogenic <u>pollution</u> emissions. For example, in 2013, the meteorological and emission impacts on $PM_{2.5}$ in the NCP region were -17.35 $\mu g/m^3$ and 4.49 $\mu g/m^3$, respectively. Similarly, in the FWP region from 2013 to 2015, meteorological impacts ranged from -16.9 to -15.36 $\mu g/m^3$, while emissions affected $PM_{2.5}$ concentrations between -15.8 and -2.27 $\mu g/m^3$. The influence of meteorology also exceeded that of emissions in the YRD region during 2011–2012 and in the PRD region in 2010. Even in the SCB region, where meteorological impacts on $PM_{2.5}$ were relatively minor, meteorological effects in 2010 (8.59 $\mu g/m^3$) were comparable to emissions (-14.67 $\mu g/m^3$).

 The influence of CO₂ concentration emission changes on PM_{2.5} levels was generally minor but, in the densely vegetated PRD region, could be comparable to the effects of emissions and meteorology. The influences of CO₂ concentration emissions, anthropogenic pollutant emissions, and meteorology on PM_{2.5} are -0.25 to 3.11 μ g/m³, -6.19 to -1.47 μ g/m³, and -0.5 to 3.11 μ g/m³, respectively from 2009 to 2013.

Our attribution analysis of PM_{2.5} concentration changes is mainly consistent with previous studies, which have indicated that variations in anthropogenic pollution emissions were the primary driver of PM_{2.5} changes in China during 2013-2017, with meteorological conditions contributing approximately 9 %-26 % (Zhang et al., 2019; Chen et al., 2020a; Cheng et al., 2019). In our study, relative to 2008, the average contribution of anthropogenic pollution emissions during the PreG period was 89.08 %, while meteorological conditions contributed 16.45 %. In the PostG period, following the implementation of the Clean Air Action Plan, the influence of anthropogenic pollution emissions further increased to 96.26 %, whereas the contribution of meteorological conditions declined to 1.60 %. This finding underscores that the impact of changes in anthropogenic pollution emissions on PM_{2.5} concentrations was markedly enhanced after 2013. Notably, changes in CO₂ concentrations emissions had a significant impact on PM_{2.5} levels, contributing -5.46 % during the PreG period and 2.14 % during the PostG period, with the latter effect surpassing that of meteorological conditions.

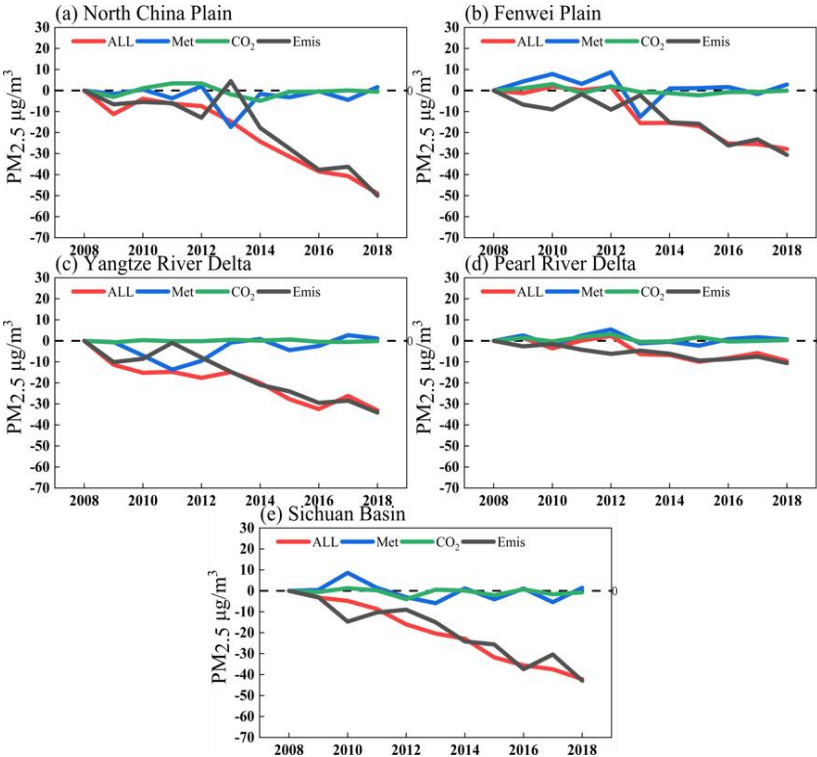


Figure 8. Changes in <u>total PM_{2.5}</u> concentrations <u>in East Asia from 2008 to 2018 (ALL, red line)</u> and the contributions of anthropogenic pollutant emissions (Emis, <u>black line</u>), meteorological conditions (Met, <u>blue line</u>), and CO₂ <u>concentration emission</u> changes (CO₂, <u>green line</u>) to PM_{2.5} concentrations <u>by Region</u> (Units: μ g/m³).

3.6 Uncertainties

The uncertainties in the MEIC emission inventory primarily arise from activity data, emission factors, spatial and temporal allocation methods, and the implementation status of pollution control measures (Hong et al., 2017; Zheng et al., 2021b), all of which may affect the accuracy of simulation results. Future improvements can be achieved by employing more refined and accurate emission inventories.

In addition, the use of a 60 km low-resolution grid limits the ability to represent local topography and physical processes, thereby introducing simulation errors (Harris et al., 2016; Ringler et al., 2013). Given that this study employs a fully coupled regional climate-chemistry-ecology model with extended simulation periods (three sets of 10-year simulations) and a broad regional scope (covering the entire East Asia region), computational resource constraints necessitated the use of 60 km grids. Numerous studies have employed the RegCM-Chem-YIBs model at a 60 km grid resolution to systematically analyze PM_{2.5}, O₃, CO₂, and the regional

climate over East Asia (Ma et al., 2023a; Ma et al., 2023b; Xu et al., 2023; Gao et al., 2021). These demonstrate its robustness and reliability in simulating East Asian atmospheric and climatic conditions. Future studies could enhance simulation accuracy by increasing computational resources and employing higher-resolution grids.

4 Conclusions

This study employed numerical experiments with the RegCM-Chem-YIBs model to analyze the interannual variability of near-surface PM_{2.5} concentrations in East Asia from 2008 to 2018. The analysis examines the drivers of annual PM_{2.5} changes in detail, focusing on three key factors: anthropogenic pollutant emissions, meteorological conditions, and CO₂ concentration-emission changes.

Compared to 2008, PM2.5 concentrations in East Asia exhibited minimal change during the PreG stage, with most areas showing variations between -10 and 5 μ g/m³. In contrast, following the implementation of the Clean Air Action Plan, PM2.5 concentrations decreased significantly during the PostG stage. This reduction was especially notable in the NCP and the SCB region, with declines of 36.76 μ g/m³ and 33.96 μ g/m³, respectively.

Anthropogenic pollutant emissions are the primary driver of the decline in $PM_{2.5}$ concentrations in East Asia, with their impact on $PM_{2.5}$ levels increasing linearly over time. During the PreG and PostG stages, the contributions of anthropogenic pollution emissions to $PM_{2.5}$ concentrations in the NCP, FWP, YRD, PRD, and SCB regions ranged from -10.39 to -3.82 μ g/m³ and -33.86 to -8.45 μ g/m³, respectively.

Changes in meteorological conditions have led to decreased $PM_{2.5}$ concentrations along China's eastern coastal and western inland regions, while increasing $PM_{2.5}$ levels in central areas. During the PreG stage, the influence of these meteorological changes on $PM_{2.5}$ concentrations was comparable to that of anthropogenic pollution emissions, ranging from -6.31 to 2.32 $\mu g/m^3$.

CO₂ indirectly influences $PM_{2.5}$ concentrations by affecting precipitation and isoprene emissions from vegetation. In the sparsely vegetated NCP and FWP regions, CO₂ impacts near-surface $PM_{2.5}$ primarily through changes in precipitation. Conversely, in the vegetation-rich PRD region, CO₂ affects $PM_{2.5}$ concentrations mainly by altering isoprene emissions, with an impact comparable to that of anthropogenic pollution emissions. From 2009 to 2013, the effects of anthropogenic pollution emissions and CO₂ changes on $PM_{2.5}$ ranged are -0.25 to 3.11 $\mu g/m^3$ and -6.19 to -1.47 $\mu g/m^3$, respectively.

In summary, PM_{2.5} concentrations in East Asia have significantly declined since 2013, primarily driven by changes in anthropogenic pollutant emissions. During several years of the PreG period, variations in meteorological conditions affected PM_{2.5} levels to a degree comparable to that of anthropogenic pollutant emissions. However, following the implementation of the Clean Air Action Plan in 2013, the influence of anthropogenic pollution emissions increased significantly, while the impact of meteorological factors diminished considerably. This simulation underscores the critical importance of stringent air pollution control measures in mitigating PM_{2.5} concentrations. Moreover, we highlight that in regions with dense vegetation cover, changes in CO₂ concentrations—emissions—play a noteworthy role in regulating PM_{2.5} levels, with the average effect during the PostG phase even surpassing that of meteorological conditions. Given the sustained rise in CO₂ levels in recent years, it is imperative to integrate the modulatory effects of CO₂ into PM_{2.5} simulating models and control strategies.

manuscript submitted to Journal of Atmospheric Chemistry and Physics

552	Data availability
553	ERA-Interim data are available at https://apps.ecmwf.int/datasets/data/interim-full-daily/ . MEIC
554	data are available at http://meicmodel.org/?page_id=560 . CarbonTracker data are available at
555	https://gml.noaa.gov/aftp/products/carbontracker/co2/CT2019/. WDCGG CO2 data are available
556	at https://gaw.kishou.go.jp/search/gas_species/co2/latest/. CNEMC_data_are_available_at_
557	http://www.cnemc.cn/. only available in Chinese, last access 1 August 2024.
558	←
559	Author contributions
560	MX, TW, and DM: designed the research, and DM: carried it out. MX, and LF: provided
561	technical support on the RegCM-Chem-YIBs mode. SZ, and SC: improved the paper. HH:
562	improved and edited the paper.
563	
564	Competing interests:
565	The contact author has declared that none of the authors has any competing interests.
566	D' L'
567	Disclaimer Publication of the p
568	Publisher's note: Copernicus Publications remains neutral with regard to jurisdictional claims in published maps and institutional affiliations.
569 570	puonsned maps and mstitutional arrinations.
571	Financial support
572	This work was supported by the National Nature Science Foundation of China (grant no.
573	42275102), the Special Science and Technology Innovation Program for Carbon Peak and
574	Carbon Neutralization of Jiangsu Province (grant no. BE2022612), and the research start-up fund
575	for the introduction of talents from Nanjing Normal University (grant no. 184080H201B57), and
576	the Special Science and Technology Innovation Program for Carbon Peak and Carbon
577	Neutralization of Jiangsu Province (BE2022612).
578	

设置了格式: 下标

带格式的: 行距: 单倍行距

References

579

582 583

584

585

586 587

588

589

590

591

592

593

594

595

596 597

598

599

600

601

602 603

604 605

606

607

608

612 613

614

615 616

617

618

619 620

621

622

623

624

- 580 Ait-Chaalal, F., Schneider, T., Meyer, B., and Marston, J. B.: Cumulant expansions for atmospheric flows, New 581 Journal of Physics, 18, 10.1088/1367-2630/18/2/025019, 2016.
 - An, Z. S., Huang, R. J., Zhang, R. Y., Tie, X. X., Li, G. H., Cao, J. J., Zhou, W. J., Shi, Z. G., Han, Y. M., Gu, Z. L., and Ji, Y. M.: Severe haze in northern China: A synergy of anthropogenic emissions and atmospheric processes, P Natl Acad Sci USA, 116, 8657-8666, 10.1073/pnas.1900125116, 2019.
 - Balsamo, G., Albergel, C., Beljaars, A., Boussetta, S., Brun, E., Cloke, H., Dee, D., Dutra, E., Munoz-Sabater, J., Pappenberger, F., de Rosnay, P., Stockdale, T., and Vitart, F.: ERA-Interim/Land: a global land surface reanalysis data set, Hydrology and Earth System Sciences, 19, 389-407, 10.5194/hess-19-389-2015, 2015.
 - Bleck, R. and Benjamin, S. G.: REGIONAL WEATHER PREDICTION WITH A MODEL COMBINING TERRAIN-FOLLOWING AND ISENTROPIC COORDINATES .1. MODEL DESCRIPTION, Monthly Weather Review, 121, 1770-1785, 10.1175/1520-0493(1993)121<1770:Rwpwam>2.0.Co;2, 1993.
 - Cao, L., Bala, G., and Caldeira, K.: Climate response to changes in atmospheric carbon dioxide and solar irradiance on the time scale of days to weeks, Environmental Research Letters, 7, 10.1088/1748-9326/7/3/034015, 2012.
 - Chen, G. B., Li, S. S., Knibbs, L. D., Hamm, N. A. S., Cao, W., Li, T. T., Guo, J. P., Ren, H. Y., Abramson, M. J., and Guo, Y. M.: A machine learning method to estimate PM_{2.5} concentrations across China with remote sensing, meteorological and land use information, Sci Total Environ, 636, 52-60, 10.1016/j.scitotenv.2018.04.251, 2018.
 - Chen, L., Zhu, J., Liao, H., Yang, Y., and Yue, X.: Meteorological influences on PM2.5 and O-3 trends and associated health burden since China's clean air actions, Sci Total Environ, 744, 10.1016/j.scitotenv.2020.140837, 2020a.
 - Chen, Z. Y., Chen, D. L., Zhao, C. F., Kwan, M. P., Cai, J., Zhuang, Y., Zhao, B., Wang, X. Y., Chen, B., Yang, J., Li, R. Y., He, B., Gao, B. B., Wang, K. C., and Xu, B.: Influence of meteorological conditions on PM_{2.5} concentrations across China: A review of methodology and mechanism, Environment International, 139, 10.1016/j.envint.2020.105558, 2020b.
 - Cheng, J., Su, J. P., Cui, T., Li, X., Dong, X., Sun, F., Yang, Y. Y., Tong, D., Zheng, Y. X., Li, Y. S., Li, J. X., Zhang, Q., and He, K. B.: Dominant role of emission reduction in PM2.5 air quality improvement in Beijing during 2013-2017: a model-based decomposition analysis, Atmospheric Chemistry and Physics, 19, 6125-6146, 10.5194/acp-19-6125-2019, 2019.
- Feng, S. L., Gao, D., Liao, F., Zhou, F. R., and Wang, X. M.: The health effects of ambient PM_{2.5} and
 potential mechanisms, Ecotoxicology and Environmental Safety, 128, 67-74, 10.1016/j.ecoenv.2016.01.030,
 2016.
 - Fontes, T., Li, P. L., Barros, N., and Zhao, P. J.: Trends of PM2.5 concentrations in China: A long term approach, Journal of Environmental Management, 196, 719-732, 10.1016/j.jenvman.2017.03.074, 2017.
 - Gao, L. B., Wang, T. J., Ren, X. J., Ma, D. Y., Zhuang, B. L., Li, S., Xie, M., Li, M. M., and Yang, X. Q.: Subseasonal characteristics and meteorological causes of surface O-3 in different East Asian summer monsoon periods over the North China Plain during 2014-2019, Atmos Environ, 264, 10.1016/j.atmosenv.2021.118704, 2021.
 - Geng, G. N., Liu, Y. X., Liu, Y., Liu, S. G., Cheng, J., Yan, L., Wu, N. N., Hu, H. W., Tong, D., Zheng, B., Yin, Z. C., He, K. B., and Zhang, Q.: Efficacy of China's clean air actions to tackle PM_{2.5} pollution between 2013 and 2020, Nature Geoscience, 17, 10.1038/s41561-024-01540-z, 2024.
 - Harris, L. M., Lin, S. J., and Tu, C. Y.: High-Resolution Climate Simulations Using GFDL HiRAM with a Stretched Global Grid, Journal of Climate, 29, 4293-4314, 10.1175/jcli-d-15-0389.1, 2016.
 - Heald, C. L., Wilkinson, M. J., Monson, R. K., Alo, C. A., Wang, G. L., and Guenther, A.: Response of isoprene emission to ambient CO2 changes and implications for global budgets, Global Change Biology, 15, 1127-1140, 10.1111/j.1365-2486.2008.01802.x, 2009.
- Hong, C. P., Zhang, Q., He, K. B., Guan, D. B., Li, M., Liu, F., and Zheng, B.: Variations of China's emission estimates: response to uncertainties in energy statistics, Atmospheric Chemistry and Physics, 17, 1227-1239, 10.5194/acp-17-1227-2017, 2017.
- Hu, B., Zhao, X. J., Liu, H., Liu, Z. R., Song, T., Wang, Y. S., Tang, L. Q., Xia, X. G., Tang, G. Q., Ji, D. S., Wen, T.
 X., Wang, L. L., Sun, Y., and Xin, J. Y.: Quantification of the impact of aerosol on broadband solar radiation in North China, Sci Rep-Uk, 7, 10.1038/srep44851, 2017.
- Huang, B. Y., Liu, C. Y., Banzon, V., Freeman, E., Graham, G., Hankins, B., Smith, T., and Zhang, H. M.:
 Improvements of the Daily Optimum Interpolation Sea Surface Temperature (DOISST) Version 2.1,
 Journal of Climate, 34, 2923-2939, 10.1175/jcli-d-20-0166.1, 2021.

- Kellomaki, S. and Wang, K. Y.: Growth, respiration and nitrogen content in needles of Scots pine exposed to elevated ozone and carbon dioxide in the field, Environmental pollution (Barking, Essex: 1987), 101, 263-274, 10.1016/s0269-7491(98)00036-0, 1998.
- Kergoat, L., Lafont, S., Douville, H., Berthelot, B., Dedieu, G., Planton, S., and Royer, J. F.: Impact of doubled CO₂ on global-scale leaf area index and evapotranspiration:: Conflicting stomatal conductance and LAI responses -: art. no. 4808, Journal of Geophysical Research-Atmospheres, 107, 10.1029/2001jd001245, 2002.
 - Kim, K. H., Kabir, E., and Kabir, S.: A review on the human health impact of airborne particulate matter, Environment International, 74, 136-143, 10.1016/j.envint.2014.10.005, 2015.

643

644

645

646

647

648 649

650

651

652

653

654 655

656

657

658

659

660

661

662

663

664

665

666

667

668

669 670

671

672

673

674

675

- Kleist, E., Mentel, T. F., Andres, S., Bohne, A., Folkers, A., Kiendler-Scharr, A., Rudich, Y., Springer, M., Tillmann, R., and Wildt, J.: Irreversible impacts of heat on the emissions of monoterpenes, sesquiterpenes, phenolic BVOC and green leaf volatiles from several tree species, Biogeosciences, 9, 5111-5123, 10.5194/bg-9-5111-2012, 2012.
- Kong, L., Tang, X., Zhu, J., Wang, Z., Li, J., Wu, H., Wu, Q., Chen, H., Zhu, L., Wang, W., Liu, B., Wang, Q., Chen, D., Pan, Y., Song, T., Li, F., Zheng, H., Jia, G., Lu, M., Wu, L., and Carmichael, G. R.: A 6-year-long (2013-2018) high-resolution air quality reanalysis dataset in China based on the assimilation of surface observations from CNEMC, Earth System Science Data, 13, 529-570, 10.5194/essd-13-529-2021, 2021.
- Kramer, A. J., Rattanavaraha, W., Zhang, Z. F., Gold, A., Surratt, J. D., and Lin, Y. H.: Assessing the oxidative potential of isoprene-derived epoxides and secondary organic aerosol, Atmos Environ, 130, 211-218, 10.1016/j.atmosenv.2015.10.018, 2016.
- Kurokawa, J. and Ohara, T.: Long-term historical trends in air pollutant emissions in Asia: Regional Emission inventory in ASia (REAS) version 3, Atmospheric Chemistry and Physics, 20, 12761-12793, 10.5194/acp-20-12761-2020, 2020.
- Lei, Y. D., Yue, X., Liao, H., Gong, C., and Zhang, L.: Implementation of Yale Interactive terrestrial Biosphere model v1.0 into GEOS-Chem v12.0.0: a tool for biosphere-chemistry interactions, Geoscientific Model Development, 13, 1137-1153, 10.5194/gmd-13-1137-2020, 2020.
- Li, G. H., Bei, N. F., Cao, J. J., Huang, R. J., Wu, J. R., Feng, T., Wang, Y. C., Liu, S. X., Zhang, Q., Tie, X. X., and Molina, L. T.: A possible pathway for rapid growth of sulfate during haze days in China, Atmospheric Chemistry and Physics, 17, 3301-3316, 10.5194/acp-17-3301-2017, 2017a.
- Li, J., Chen, X. S., Wang, Z. F., Du, H. Y., Yang, W. Y., Sun, Y. L., Hu, B., Li, J. J., Wang, W., Wang, T., Fu, P. Q., and Huang, H. L.: Radiative and heterogeneous chemical effects of aerosols on ozone and inorganic aerosols over East Asia, Sci Total Environ, 622, 1327-1342, 10.1016/j.scitotenv.2017.12.041, 2018.
- Li, K., Jacob, D. J., Liao, H., Zhu, J., Shah, V., Shen, L., Bates, K. H., Zhang, Q., and Zhai, S. X.: A two-pollutant strategy for improving ozone and particulate air quality in China, Nature Geoscience, 12, 906-+, 10.1038/s41561-019-0464-x, 2019.
- Li, X., Feng, Y. J., Liang, H. Y., and Iop: The Impact of Meteorological Factors on PM2.5 Variations in Hong Kong, 8th International Conference on Environmental Science and Technology (ICEST), Technical University Of Madrid, Computer Science School, madrid, SPAIN, Jun 12-14, WOS:000440342600003, 10.1088/1755-1315/78/1/012003, 2017.
- Li, Z. and Mölders, N.: Interaction of impacts of doubling CO₂ and changing regional land-cover on evaporation, precipitation, and runoff at global and regional scales, International Journal of Climatology, 28, 1653-1679, 10.1002/joc.1666, 2008.
- Lin, C. Q., Liu, G., Lau, A. K. H., Li, Y., Li, C. C., Fung, J. C. H., and Lao, X. Q.: High-resolution satellite remote sensing of provincial PM_{2.5} trends in China from 2001 to 2015, Atmos Environ, 180, 110-116, 10.1016/j.atmosenv.2018.02.045, 2018.
- Lin, Y. H., Knipping, E. M., Edgerton, E. S., Shaw, S. L., and Surratt, J. D.: Investigating the influences of SO
 sub>2
 sub>3
 sub>1
 evels on isoprene-derived secondary organic aerosol formation using conditional sampling approaches, Atmospheric Chemistry and Physics, 13, 8457-8470, 10.5194/acp-13-8457-2013, 2013.
- Lindwall, F., Schollert, M., Michelsen, A., Blok, D., and Rinnan, R.: Fourfold higher tundra volatile emissions due
 to arctic summer warming, Journal of Geophysical Research-Biogeosciences, 121, 895-902,
 10.1002/2015jg003295, 2016.
- Ma, D., Wang, T., Wu, H., Qu, Y., Liu, J., Liu, J., Li, S., Zhuang, B., Li, M., and Xie, M.: The effect of anthropogenic emission, meteorological factors, and carbon dioxide on the surface ozone increase in China from 2008 to 2018 during the East Asia summer monsoon season, Atmos. Chem. Phys., 23, 6525-6544,
 10.5194/acp-23-6525-2023, 2023a.

- Ma, D. Y., Wang, T. J., Xu, B. Y., Song, R., Gao, L. B., Chen, H. M., Ren, X. J., Li, S., Zhuang, B. L., Li, M. M., Xie,
 M., and Saikawa, E.: The mutual interactions among ozone, fine particulate matter, and carbon dioxide on
 summer monsoon climate in East Asia, Atmos Environ, 299, 10.1016/j.atmosenv.2023.119668, 2023b.
- 694 Ma, Z., Liu, R., Liu, Y., and Bi, J.: Effects of air pollution control policies on PM_{2.5} pollution improvement in China from 2005 to 2017: a satellite-based perspective, Atmospheric Chemistry and Physics, 19, 6861-6877, 10.5194/acp-19-6861-2019, 2019.

698

699

700

701

702

703

704

705

706

707

708

709

710

711

712

713

714

715

716

717

718

719

720

721

722

723

724

725

726

727

728

729

730 731

732

733

734

735

736 737

738

- Ma, Z. W., Hu, X. F., Sayer, A. M., Levy, R., Zhang, Q., Xue, Y. G., Tong, S. L., Bi, J., Huang, L., and Liu, Y.: Satellite-Based Spatiotemporal Trends in PM2.5 Concentrations: China, 2004-2013, Environmental Health Perspectives, 124, 184-192, 10.1289/ehp.1409481, 2016.
- Matthews, H. D.: Implications of CO₂ fertilization for future climate change in a coupled climate-carbon model, Global Change Biology, 13, 1068-1078, 10.1111/j.1365-2486.2007.01343.x, 2007.
- Mousavinezhad, S., Choi, Y., Pouyaei, A., Ghahremanloo, M., and Nelson, D. L.: A comprehensive investigation of surface ozone pollution in China, 2015-2019: Separating the contributions from meteorology and precursor emissions, Atmospheric Research, 257, 10.1016/j.atmosres.2021.105599, 2021.
- Pan, L., Xu, J. M., Tie, X. X., Mao, X. Q., Gao, W., and Chang, L. Y.: Long-term measurements of planetary boundary layer height and interactions with PM_{2.5} in Shanghai, China, Atmospheric Pollution Research, 10, 989-996, 10.1016/j.apr.2019.01.007, 2019.
- Pegoraro, E., Rey, A., Bobich, E. G., Barron-Gafford, G., Grieve, K. A., Malhi, Y., and Murthy, R.: Effect of elevated CO₂ concentration and vapour pressure deficit on isoprene emission from leaves of <i>Populus</i> <i>deltoides</i> during drought, Functional Plant Biology, 31, 1137-1147, 10.1071/fp04142, 2004.
- Peters, W., Jacobson, A. R., Sweeney, C., Andrews, A. E., Conway, T. J., Masarie, K., Miller, J. B., Bruhwiler, L. M. P., Petron, G., Hirsch, A. I., Worthy, D. E. J., van der Werf, G. R., Randerson, J. T., Wennberg, P. O., Krol, M. C., and Tans, P. P.: An atmospheric perspective on North American carbon dioxide exchange: CarbonTracker, P Natl Acad Sci USA, 104, 18925-18930, 10.1073/pnas.0708986104, 2007.
- Possell, M., Hewitt, C. N., and Beerling, D. J.: The effects of glacial atmospheric CO2 concentrations and climate on isoprene emissions by vascular plants, Global Change Biology, 11, 60-69, 10.1111/j.1365-2486.2004.00889.x, 2005.
- Pui, D. Y. H., Chen, S. C., and Zuo, Z. L.: PM2.5 in China: Measurements, sources, visibility and health effects, and mitigation, Particuology, 13, 1-26, 10.1016/j.partic.2013.11.001, 2014.
- Ringler, T., Petersen, M., Higdon, R. L., Jacobsen, D., Jones, P. W., and Maltrud, M.: A multi-resolution approach to global ocean modeling, Ocean Modelling, 69, 211-232, 10.1016/j.ocemod.2013.04.010, 2013.
- Shalaby, A., Zakey, A. S., Tawfik, A. B., Solmon, F., Giorgi, F., Stordal, F., Sillman, S., Zaveri, R. A., and Steiner, A. L.: Implementation and evaluation of online gas-phase chemistry within a regional climate model (RegCM-CHEM4), Geoscientific Model Development, 5, 741-760, 10.5194/gmd-5-741-2012, 2012.
- Silver, B., Reddington, C. L., Arnold, S. R., and Spracklen, D. V.: Substantial changes in air pollution across China during 2015-2017, Environmental Research Letters, 13, 10.1088/1748-9326/aae718, 2018.
- Silver, B., Reddington, C. L., Chen, Y., and Arnold, S. R.: A decade of China's air quality monitoring data suggests health impacts are no longer declining, Environment International, 197, 10.1016/j.envint.2025.109318, 2025.
- Sun, Z. H., Hve, K., Vislap, V., and Niinemets, U.: Elevated CO2 magnifies isoprene emissions under heat and improves thermal resistance in hybrid aspen, Journal of Experimental Botany, 64, 5509-5523, 10.1093/jxb/ert318, 2013.
- Sun, Z. H., Niinemets, Ü., Hüve, K., Noe, S. M., Rasulov, B., Copolovici, L., and Vislap, V.: Enhanced isoprene emission capacity and altered light responsiveness in aspen grown under elevated atmospheric CO2 concentration, Global Change Biology, 18, 3423-3440, 10.1111/j.1365-2486.2012.02789.x, 2012.
- van Donkelaar, A., Martin, R. V., Li, C., and Burnett, R. T.: Regional Estimates of Chemical Composition of Fine Particulate Matter Using a Combined Geoscience-Statistical Method with Information from Satellites, Models, and Monitors, Environmental Science & Technology, 53, 2595-2611, 10.1021/acs.est.8b06392, 2019.
- 740 2019.
 741 van Donkelaar, A., Martin, R. V., Brauer, M., Kahn, R., Levy, R., Verduzco, C., and Villeneuve, P. J.: Global
 742 Estimates of Ambient Fine Particulate Matter Concentrations from Satellite-Based Aerosol Optical Depth:
 743 Development and Application, Environmental Health Perspectives, 118, 847-855, 10.1289/ehp.0901623,
 744 2010.
- Vu, T. V., Shi, Z. B., Cheng, J., Zhang, Q., He, K. B., Wang, S. X., and Harrison, R. M.: Assessing the impact of
 clean air action on air quality trends in Beijing using a machine learning technique, Atmospheric Chemistry

- 747 and Physics, 19, 11303-11314, 10.5194/acp-19-11303-2019, 2019.
 - Wang, H., Peng, Y., Zhang, X. Y., Liu, H. L., Zhang, M., Che, H. Z., Cheng, Y. L., and Zheng, Y.: Contributions to the explosive growth of PM2.5 mass due to aerosol-radiation feedback and decrease in turbulent diffusion during a red alert heavy haze in Beijing-Tianjin-Hebei, China, Atmospheric Chemistry and Physics, 18, 17717-17733, 10.5194/acp-18-17717-2018, 2018a.
 - Wang, H. B., Tian, M., Chen, Y., Shi, G. M., Liu, Y., Yang, F. M., Zhang, L. M., Deng, L. Q., Yu, J., Peng, C., and Cao, X. Y.: Seasonal characteristics, formation mechanisms and source origins of PM_{2.5} in two megacities in Sichuan Basin, China, Atmospheric Chemistry and Physics, 18, 865-881, 10.5194/acp-18-865-2018, 2018b.
 - Wang, J. D., Zhao, B., Wang, S. X., Yang, F. M., Xing, J., Morawska, L., Ding, A. J., Kulmala, M., Kerminen, V. M., Kujansuu, J., Wang, Z. F., Ding, D. A., Zhang, X. Y., Wang, H. B., Tian, M., Petaja, T., Jiang, J. K., and Hao, J. M.: Particulate matter pollution over China and the effects of control policies, Sci Total Environ, 584, 426-447, 10.1016/j.scitotenv.2017.01.027, 2017.
 - Wei, J., Li, Z. Q., Lyapustin, A., Sun, L., Peng, Y. R., Xue, W. H., Su, T. N., and Cribb, M.: Reconstructing 1-km-resolution high-quality PM2.5 data records from 2000 to 2018 in China: spatiotemporal variations and policy implications, Remote Sens Environ, 252, ARTN 112136
 - 10.1016/j.rse.2020.112136, 2021.

749

750

751

752

753

754

755

756 757

758

759

760

761

762

763

764

765

766 767

768

769 770

771

772

773

774

775 776

777

778

779

780

781

782 783

784

785 786

787

788

789

790

791

792

793

797

798

- Wilkinson, M. J., Monson, R. K., Trahan, N., Lee, S., Brown, E., Jackson, R. B., Polley, H. W., Fay, P. A., and Fall, R.: Leaf isoprene emission rate as a function of atmospheric CO2 concentration, Global Change Biology, 15, 1189-1200, 10.1111/j.1365-2486.2008.01803.x, 2009.
- Wu, H., Wang, T. J., Wang, Q., Cao, Y., Qu, Y. W., and Nie, D. Y.: Radiative effects and chemical compositions of fine particles modulating urban heat island in Nanjing, China, Atmos Environ, 247, 10.1016/j.atmosenv.2021.118201, 2021.
- Wu, K., Yang, X. Y., Chen, D., Gu, S., Lu, Y. Q., Jiang, Q., Wang, K., Ou, Y. H., Qian, Y., Shao, P., and Lu, S. H.: Estimation of biogenic VOC emissions and their corresponding impact on ozone and secondary organic aerosol formation in China, Atmospheric Research, 231, 10.1016/j.atmosres.2019.104656, 2020.
- Wu, Y. N., Liu, J. K., Zhai, J. X., Cong, L., Wang, Y., Ma, W. M., Zhang, Z. M., and Li, C. Y.: Comparison of dry and wet deposition of particulate matter in near-surface waters during summer, Plos One, 13, 10.1371/journal.pone.0199241, 2018.
- Xiao, Q. Y., Zheng, Y. X., Geng, G. N., Chen, C. H., Huang, X. M., Che, H. Z., Zhang, X. Y., He, K. B., and Zhang, Q.: Separating emission and meteorological contributions to long-term PM_{2.5} trends over eastern China during 2000-2018, Atmospheric Chemistry and Physics, 21, 9475-9496, 10.5194/acp-21-9475-2021, 2021.
- Xie, N. H., Wang, T. J., Xie, X. D., Yue, X., Giorgi, F., Zhang, Q., Ma, D. Y., Song, R., Xu, B. Y., Li, S., Zhuang, B. L., Li, M. M., Xie, M., Kilifarska, N. A., Gadzhev, G., and Dimitrova, R.: The regional climate-chemistry-ecology coupling model RegCM-Chem (v4.6)-YIBs (v1.0): development and application, Geoscientific Model Development, 17, 3259-3277, 10.5194/gmd-17-3259-2024, 2024.
- Xie, X., Wang, T., Yue, X., Li, S., Zhuang, B., Wang, M., and Yang, X.: Numerical modeling of ozone damage to plants and its effects on atmospheric CO2 in China, Atmospheric Environment, 217, 10.1016/j.atmosenv.2019.116970, 2019.
- Xing, Y. F., Xu, Y. H., Shi, M. H., and Lian, Y. X.: The impact of PM2.5 on the human respiratory system, Journal of Thoracic Disease, 8, E69-E74, 10.3978/j.issn.2072-1439.2016.01.19, 2016.
- Xu, B. Y., Wang, T. J., Ma, D. Y., Song, R., Zhang, M., Gao, L. B., Li, S., Zhuang, B. L., Li, M. M., and Xie, M.: Impacts of regional emission reduction and global climate change on air quality and temperature to attain carbon neutrality in China, Atmospheric Research, 279, 10.1016/j.atmosres.2022.106384, 2022.
- Xu, B. Y., Wang, T. J., Gao, L. B., Ma, D. Y., Song, R., Zhao, J., Yang, X. G., Li, S., Zhuang, B. L., Li, M. M., and Xie, M.: Impacts of meteorological factors and ozone variation on crop yields in China concerning carbon neutrality objectives in 2060, Environmental Pollution, 317, 10.1016/j.envpol.2022.120715, 2023.
- neutrality objectives in 2060, Environmental Pollution, 317, 10.1016/j.envpol.2022.120715, 2023.
 Xue, W. H., Zhang, J., Zhong, C., Ji, D. Y., and Huang, W.: Satellite-derived spatiotemporal PM2.5 concentrations and variations from 2006 to 2017 in China, Sci Total Environ, 712, 10.1016/j.scitotenv.2019.134577, 2020.
 - Yue, X. and Unger, N.: The Yale Interactive terrestrial Biosphere model version 1.0: description, evaluation and implementation into NASA GISS ModelE2, Geoscientific Model Development, 8, 2399-2417, 10.5194/gmd-8-2399-2015, 2015.
- Yue, X., Unger, N., and Zheng, Y.: Distinguishing the drivers of trends in land carbon fluxes and plant volatile
 emissions over the past 3 decades, Atmospheric Chemistry and Physics, 15, 11931-11948, 10.5194/acp-15 11931-2015, 2015.

manuscript submitted to Journal of Atmospheric Chemistry and Physics

Zhai, S. X., Jacob, D. J., Wang, X., Shen, L., Li, K., Zhang, Y. Z., Gui, K., Zhao, T. L., and Liao, H.: Fine particulate
 matter (PM2.5) trends in China, 2013-2018: separating contributions from anthropogenic emissions and
 meteorology, Atmospheric Chemistry and Physics, 19, 11031-11041, 10.5194/acp-19-11031-2019, 2019.

 $\begin{array}{c} 812 \\ 813 \end{array}$

- Zhang, B. E., Jiao, L. M., Xu, G., Zhao, S. L., Tang, X., Zhou, Y., and Gong, C.: Influences of wind and precipitation on different-sized particulate matter concentrations (PM_{2.5}, PM₁₀, PM_{2.5-10}), Meteorol Atmos Phys, 130, 383-392, 10.1007/s00703-017-0526-9, 2018.
- Zhang, Q., Zheng, Y. X., Tong, D., Shao, M., Wang, S. X., Zhang, Y. H., Xu, X. D., Wang, J. N., He, H., Liu, W. Q., Ding, Y. H., Lei, Y., Li, J. H., Wang, Z. F., Zhang, X. Y., Wang, Y. S., Cheng, J., Liu, Y., Shi, Q. R., Yan, L., Geng, G. N., Hong, C. P., Li, M., Liu, F., Zheng, B., Cao, J. J., Ding, A. J., Gao, J., Fu, Q. Y., Huo, J. T., Liu, B. X., Liu, Z. R., Yang, F. M., He, K. B., and Hao, J. M.: Drivers of improved PM2.5 air quality in China from 2013 to 2017, P Natl Acad Sci USA, 116, 24463-24469, 10.1073/pnas.1907956116, 2019.
- Zhang, Y., Olsen, K. M., and Wang, K.: Fine Scale Modeling of Agricultural Air Quality over the Southeastern United States Using Two Air Quality Models. Part I. Application and Evaluation, Aerosol and Air Quality Research, 13, 1231-1252, 10.4209/aaqr.2012.12.0346, 2013.
- Zhang, Y., Gentine, P., Luo, X. Z., Lian, X., Liu, Y. L., Zhou, S., Michalak, A. M., Sun, W., Fisher, J. B., Piao, S. L., and Keenan, T. F.: Increasing sensitivity of dryland vegetation greenness to precipitation due to rising atmospheric CO₂, Nature Communications, 13, 10.1038/s41467-022-32631-3, 2022.
- Zheng, B., Zhang, Q., Geng, G. N., Chen, C. H., Shi, Q. R., Cui, M. S., Lei, Y., and He, K. B.: Changes in China's anthropogenic emissions and air quality during the COVID-19 pandemic in 2020, Earth System Science Data, 13, 2895-2907, 10.5194/essd-13-2895-2021, 2021a.
- Zheng, B., Cheng, J., Geng, G. N., Wang, X., Li, M., Shi, Q. R., Qi, J., Lei, Y., Zhang, Q., and He, K. B.: Mapping anthropogenic emissions in China at 1 km spatial resolution and its application in air quality modeling, Science Bulletin, 66, 612-620, 10.1016/j.scib.2020.12.008, 2021b.
- Zheng, B., Tong, D., Li, M., Liu, F., Hong, C. P., Geng, G. N., Li, H. Y., Li, X., Peng, L. Q., Qi, J., Yan, L., Zhang, Y. X., Zhao, H. Y., Zheng, Y. X., He, K. B., and Zhang, Q.: Trends in China's anthropogenic emissions since 2010 as the consequence of clean air actions, Atmospheric Chemistry and Physics, 18, 14095-14111, 10.5194/acp-18-14095-2018, 2018.
- Zhong, J. T., Zhang, X. Y., Dong, Y. S., Wang, Y. Q., Liu, C., Wang, J. Z., Zhang, Y. M., and Che, H. C.: Feedback effects of boundary-layer meteorological factors on cumulative explosive growth of PM_{2.5} during winter heavy pollution episodes in Beijing from 2013 to 2016, Atmospheric Chemistry and Physics, 18, 247-258, 10.5194/acp-18-247-2018, 2018.

Page 29 of 29